Neutron scattering and (n, charged particle) measurements

[Arnd Junghans]
Helmholtz-Zentrum Dresden-Rossendorf
Germany

Table of Content

- from yesterday's lecture: Neutrons for Science facility at SPIRAL-2
- Relevance of inelastic scattering and neutron-induced charge-particle reactions
- nELBE experiments on inelastic scattering ^{56}Fe
- GAINS experiments on inelastic scattering ^{56}Fe
- Neutron-induced charged particle reactions ^{26}Al

The Neutrons For Science facility at SPIRAL-2

X. Ledoux and the NFS collaboration

Description

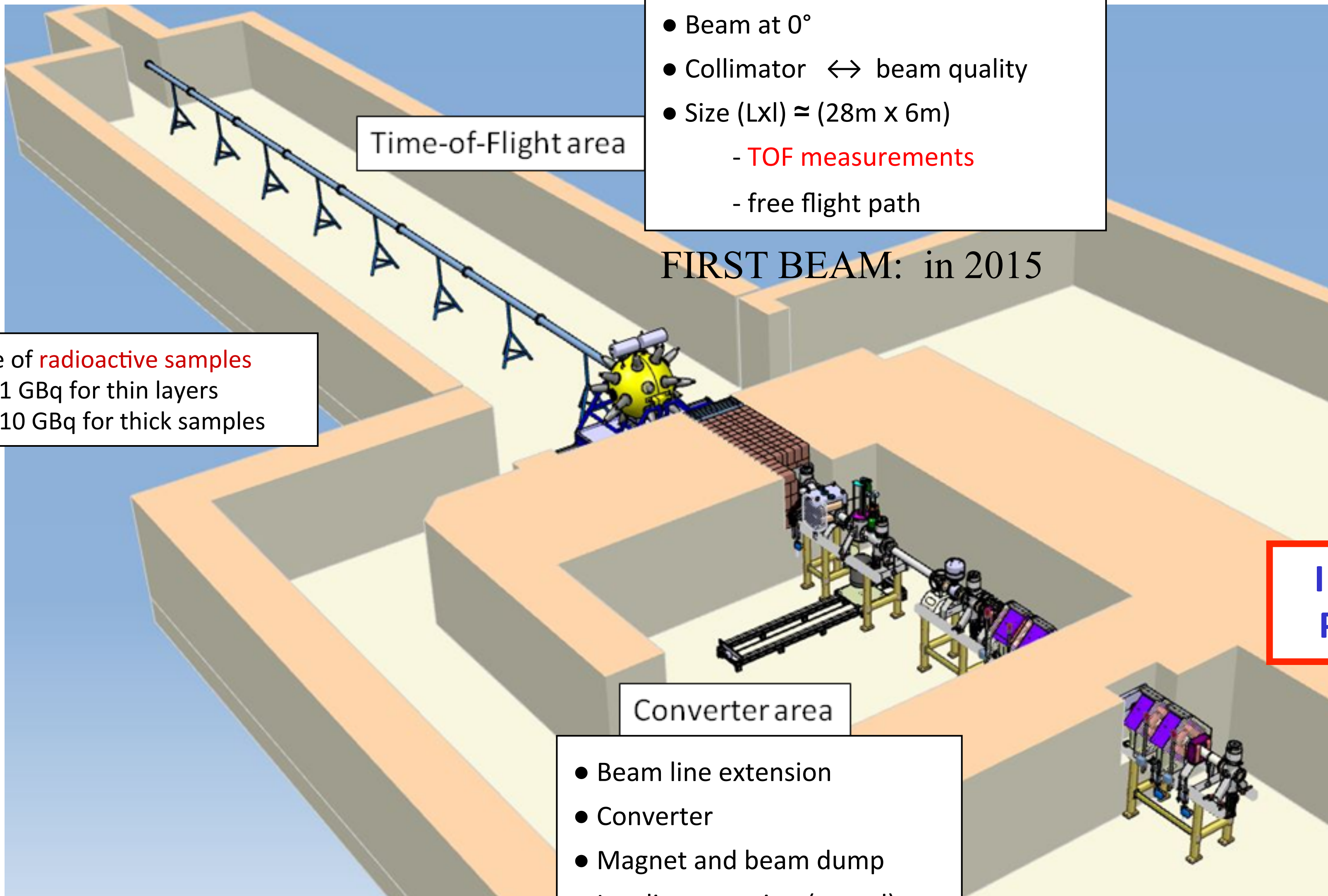

- Beam at 0°
- Collimator ↔ beam quality
- Size (Lxl) ≃ (28m x 6m)
  - TOF measurements
  - free flight path

FIRST BEAM: in 2015

Use of radioactive samples
A< 1 GBq for thin layers
A< 10 GBq for thick samples

- Beam line extension
- Converter
- Magnet and beam dump
- Irradiaton station (n, p, d)

I < 50 µA
P < 2 kW

Neutron spectra provided at NFS

Characteristics of the beams the LINAG :

- 40 MeV deuteron and 33 MeV proton
- I_{max} = 5 mA
- Pulsed beam F_0 = 88 MHz T=11 ns Burst width = 200 ps

Continuous spectrum :

E_{max} = 40 MeV , <E> = 14 MeV

thick converter (1cm)

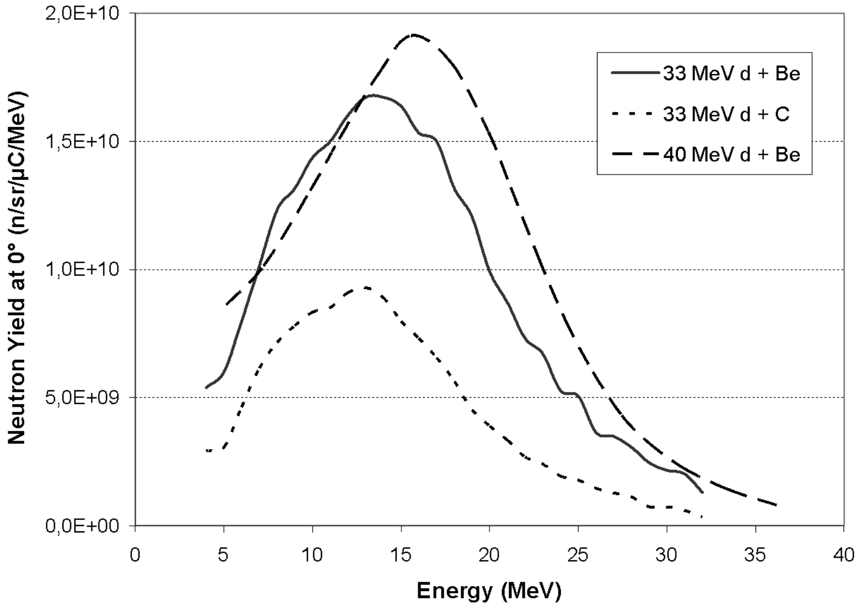

J. P. Meulders et al., Phys. Med. Biol. (1975)vol 20 n°2, p235

M. J. Saltmarsh et al., NIMA145 (1977) p81-90

Quasi-monokinetic beam :

E_n = up to 31 MeV

Thin converter (1-3 mm)

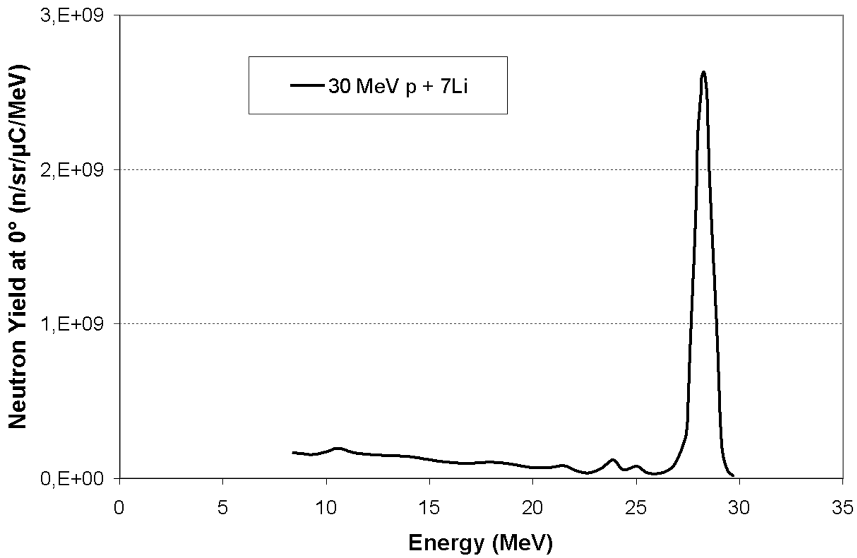

C. J. Batty et al.,NIM **68** (1969) p273-276

⇒ Similar to IFMIF spectrum

Single bunch selector for time-of-flight measurements:
Repetition rate: 150 kHz – 1 MHz

Neutron flux in the TOF area

NFS : 40 MeV d + Be

WNR : Los Alamos

n-TOF 2 : CERN

n-TOF 1 : CERN

GELINA : Geel

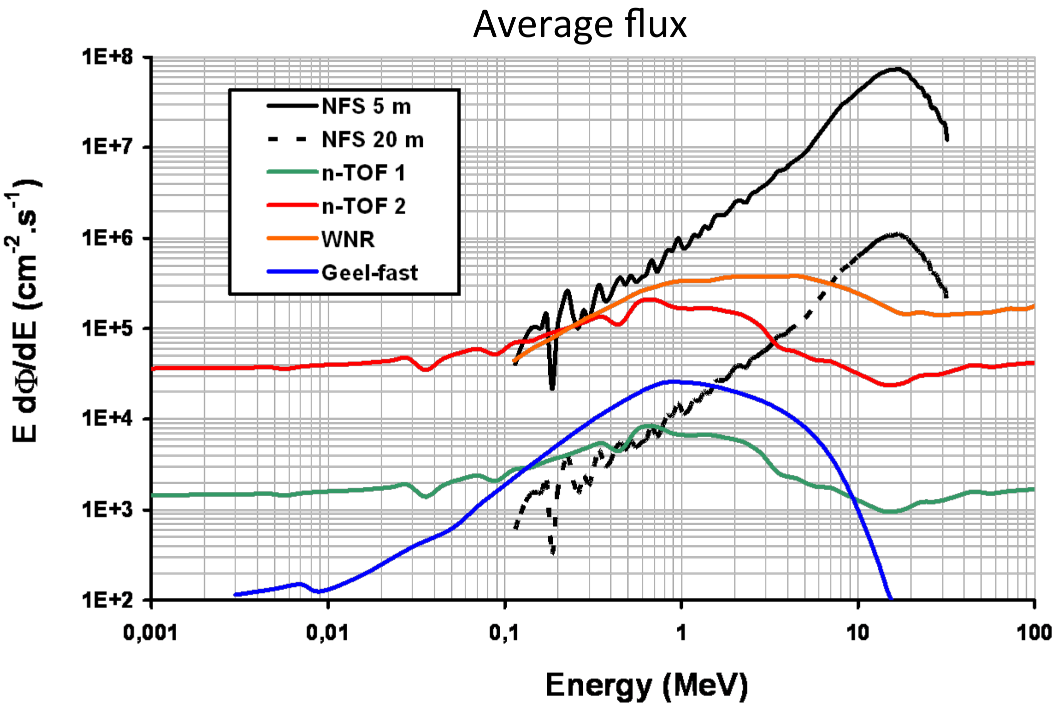

- E_n: from 0,1 MeV to 40 MeV
- Good energy resolution
- Reduced γ flash
- Low instantaneous flux

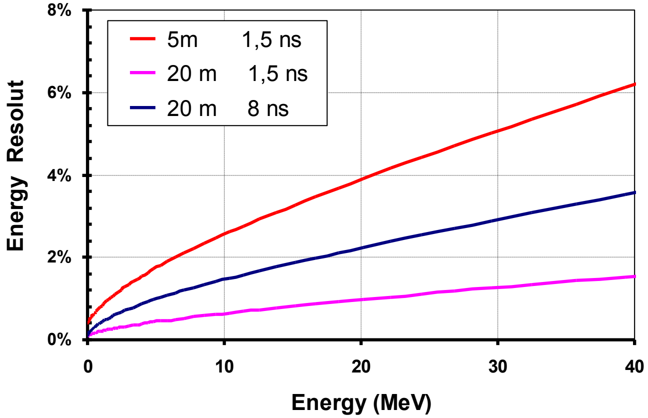

Complementary to the existing facilities

Neutron-induced reactions on ^{56}Fe

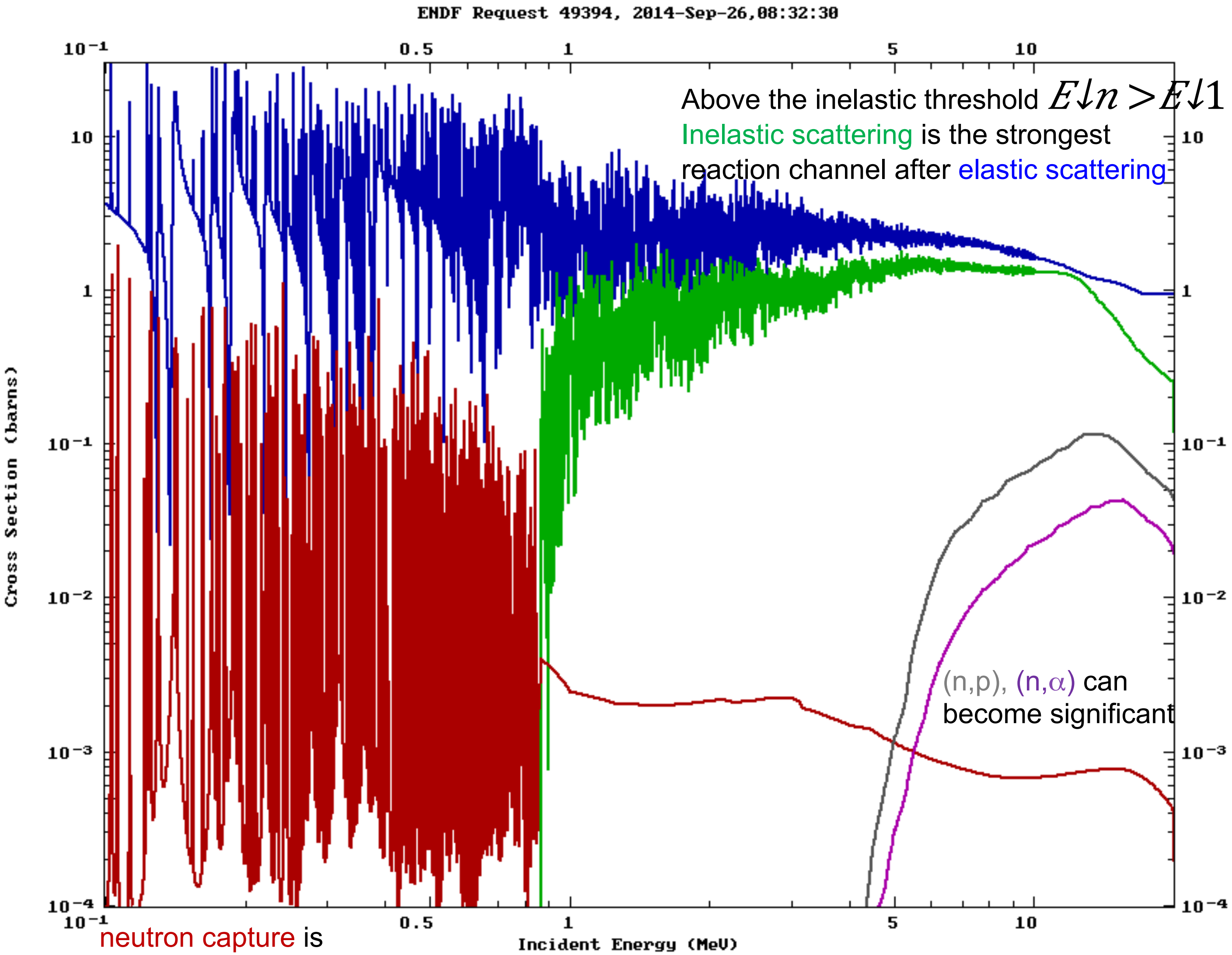

Above the inelastic threshold $E_n > E_1^*$
Inelastic scattering is the strongest reaction channel after elastic scattering

(n,p), (n,α) can become significant

neutron capture is relevant below the inelastic threshold $E_n < E_1^*$

(n,p), (n,α),… reactions are difficult to measure:

thin target required to allow emission of charged particles

activation methods as an Alternative

Data needs for fast reactors and ADS

NEA Working Party on International Nuclear Data Evaluation Co-operation (WPEC) subgroup 26

Sensitivity study of integral reactor parameters (k_{eff},...) with ERANOS fast reactor code

Table 32. Summary of Highest Priority Target Accuracies for Fast Reactors

		Energy Range	Current Accuracy (%)	Target Accuracy (%)
U238	σ_{inel}	6.07 ÷ 0.498 MeV	10 ÷ 20	2 ÷ 3
	σ_{capt}	24.8 ÷ 2.04 keV	3 ÷ 9	1.5 ÷ 2
Pu241	σ_{fiss}	1.35MeV ÷ 454 eV	8 ÷ 20	2 ÷ 3 (SFR,GFR, LFR) 5 ÷ 8 (ABTR, EFR)
Pu239	σ_{capt}	498 ÷ 2.04 keV	7 ÷ 15	4 ÷ 7
Pu240	σ_{fiss}	1.35 ÷ 0.498 MeV	6	1.5 ÷ 2
	ν	1.35 ÷ 0.498 MeV	4	1 ÷ 3
Pu242	σ_{fiss}	2.23 ÷ 0.498 MeV	19 ÷ 21	3 ÷ 5
Pu238	σ_{fiss}	1.35 ÷ 0.183 MeV	17	3 ÷ 5
Am242m	σ_{fiss}	1.35MeV ÷ 67.4keV	17	3 ÷ 4
Am241	σ_{fiss}	6.07 ÷ 2.23 MeV	12	3
Cm244	σ_{fiss}	1.35 ÷ 0.498 MeV	50	5
Cm245	σ_{fiss}	183 ÷ 67.4 keV	47	7
Fe56	σ_{inel}	2.23 ÷ 0.498 MeV	16 ÷ 25	3 ÷ 6
Na23	σ_{inel}	1.35 ÷ 0.498 MeV	28	4 ÷ 10
Pb206	σ_{inel}	2.23 ÷ 1.35 MeV	14	3
Pb207	σ_{inel}	1.35 ÷ 0.498 MeV	11	3
Si28	σ_{inel}	6.07 ÷ 1.35 MeV	14 ÷ 50	3 ÷ 6
	σ_{capt}	19.6 ÷ 6.07 MeV	53	6

Table 20. Fast reactor and ADMAB target accuracies (1σ)

Multiplication factor (BOL)	300 pcm
Power peak (BOL)	2%
Burn-up reactivity swing	300 pcm
Reactivity coefficients (coolant void and Doppler – BOL)	7%
Major nuclide density at end of irradiation cycle	2%
Other nuclide density at end of irradiation cycle	10%

➔ fast neutron spectrum

➔ U,Pu + minor actinides structural & coolant materials

- neutron induced fission
- neutron capture
- neutron inelastic scattering

➔ U,Pb,Fe,Na

MCNP 6 benchmark calculations with integral experiments

Comparison of Calculation and Experiment of criticality in many integral experiments

Low enriched uranium, thermal spectrum

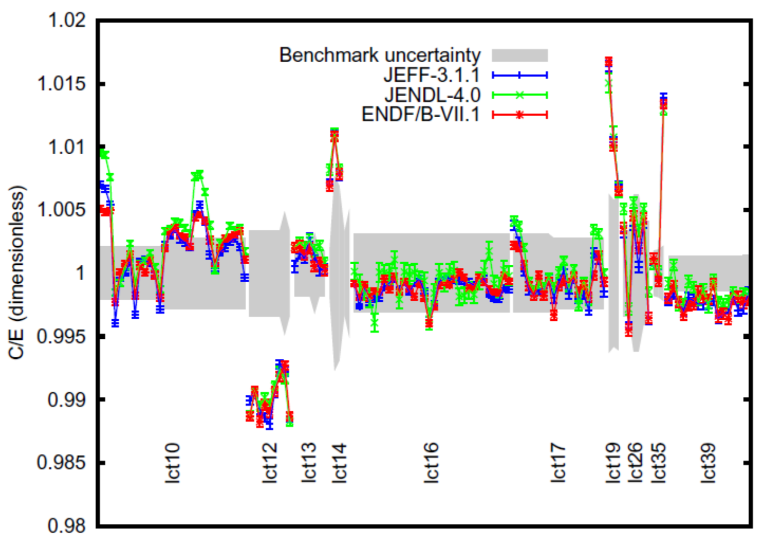

FIG. 10: Results for the LEU benchmarks with a thermal spectrum (continued).

plutonium, fast /mixed spectra

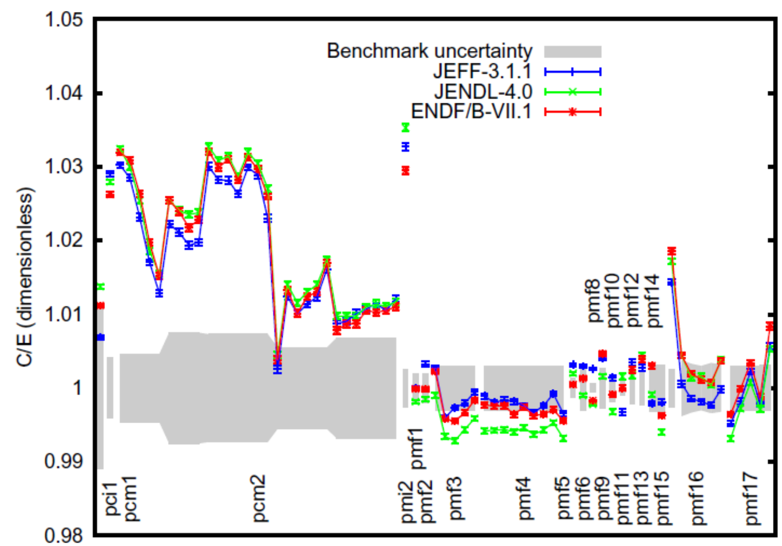

FIG. 13: Results for the PU benchmarks with a fast, intermediate, or mixed spectrum.

Analysis of criticality experiments shows requirements for improved nuclear data
JEFF-3.1.1 Joint Evaluated Fission Fusion File (OECD-NEA)
JENDL-4.0 Japanese Evaluated Nuclear Data Library
ENDF/B-VII.1 Evaluated Nuclear Data File (U.S.A.)

source: [S.C. van der Marck, Nucl. Data Sheets 113 (2013) 2935]

Neutron-induced charged particle reactions relevant to nuclear astrophysics and nuclear applications

- $^{14}N(n,p)^{14}C$ neutron poison in the transition from CNO to s-process
  (also the source of 14C production in the atmossphere, carbon dating…)
- $^{17}O(n,\alpha)^{14}C$ neutron poison for the s-process, bottleneck in inhomogeneous BBN, neutrino-driven wind r-process
  (at thermal energy both reactions produce ^{14}C from nuclear reactors)
- $^{26}Al(n,p)^{23}Na$ destruction of ^{26}Al (cosmic gamma-ray emitter)
- $^{25}Mg(n,\alpha)^{22}Ne$ neutron poison in the s-process
- $^{33}S(n,\alpha)^{30}Si$ nucleosynthesis of sulfur in explosive carbon burning
- $W(n,xn\gamma)$ fusion reactor material, low activation steels
- $^{59}Ni(n,\alpha)$ CVD Diamond detector development
- $^{239}Pu(n,2n)$ Carmen Gd Lq. Scint. Ball
- $^{16}O(n,\alpha)$ EAMEA, LPC Caen

- References: work by the nTOF collaboration and at IRMM, Gelina Grapheme setup (IPHC Strasbourg), CEA, NFS Ganil

Neutron-induced charged particle reactions relevant to nuclear astrophysics

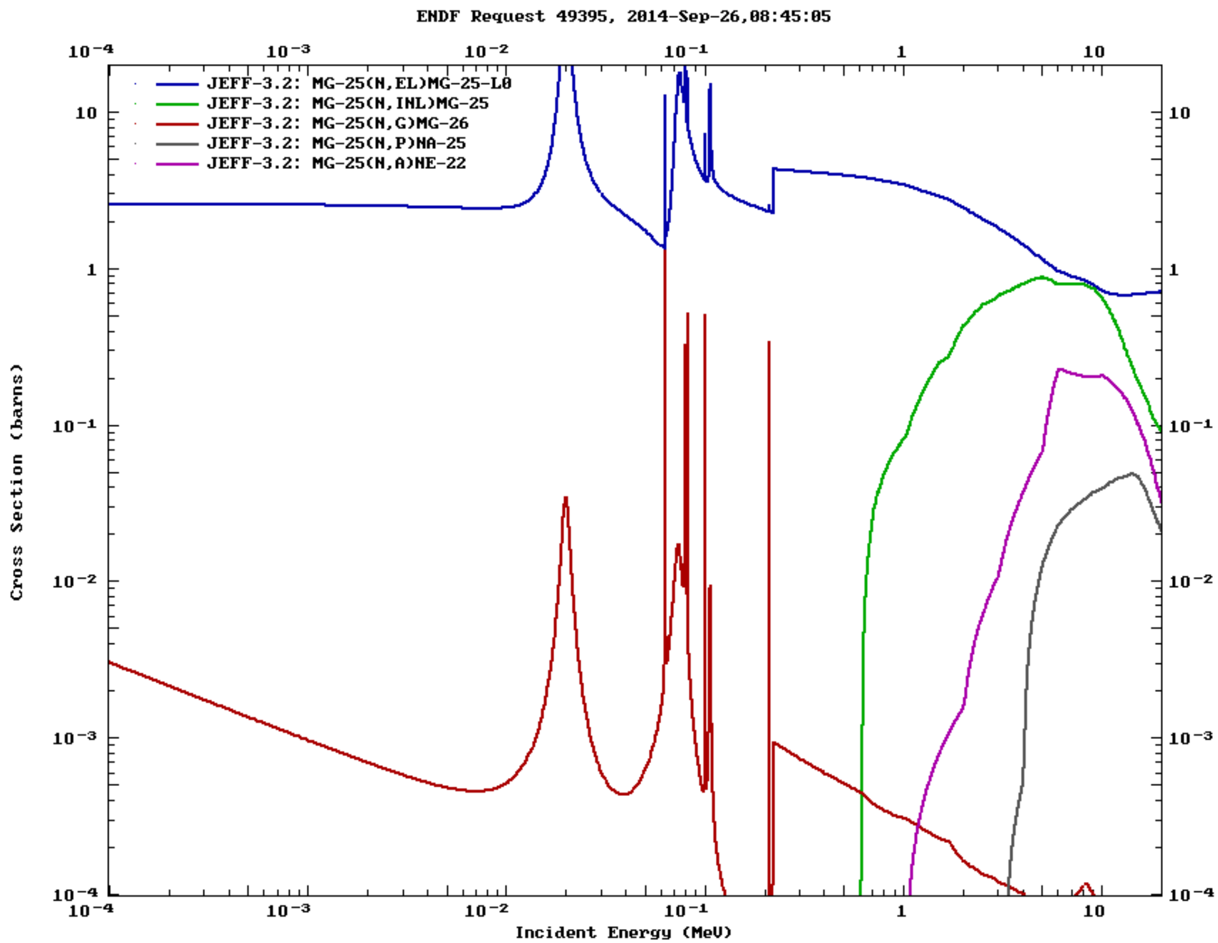

Main neutron source for the s-process: $^{22}Ne(\alpha,n)^{25}Mg$

→ $^{25}Mg(n,\alpha)$ is a neutron poison for the s-process

Q-values of neutron-induced charged particle reactions

	Q(n,p) (MeV)	Q(n,α) (MeV)
^{14}N	0.626	-0.158
^{17}O	-7.898	1.818
^{22}Na	3.625	1.951
^{25}Mg	-3.053	0.478
^{26}Al	4.787	2.966
^{33}S	0.534	3.993
^{56}Fe	-2.913	0.326
^{208}Pb	-4.217	6.185
^{238}U	-2.678	8.700

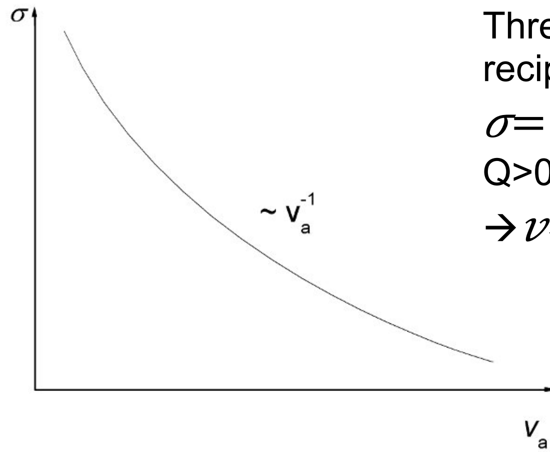

Threshold behaviour from reciprocity theorem:

$\sigma = const. v_b / v_a$

Q>0, Q≈1 MeV, E_n=1eV

$\rightarrow v_b = const. \quad \sigma \sim 1/v_a$

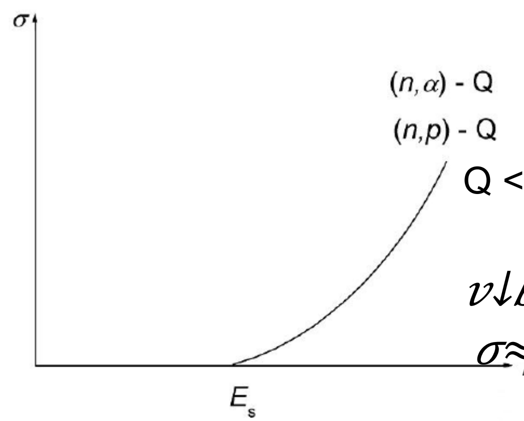

Q < 0

$\rightarrow v_a = const.$

$v_b \approx \sqrt{2 m_b (E_a - E_s)}$

$\sigma \approx \sqrt{2 m_b (E_a - E_s)}$ e

Depending on the Q-value the reactions have a threshold or not.
Q-value influenced by neutron excess and even-odd effect in neutron binding

Measurements of photon production cross section $^{56}Fe(n,n'\gamma)$

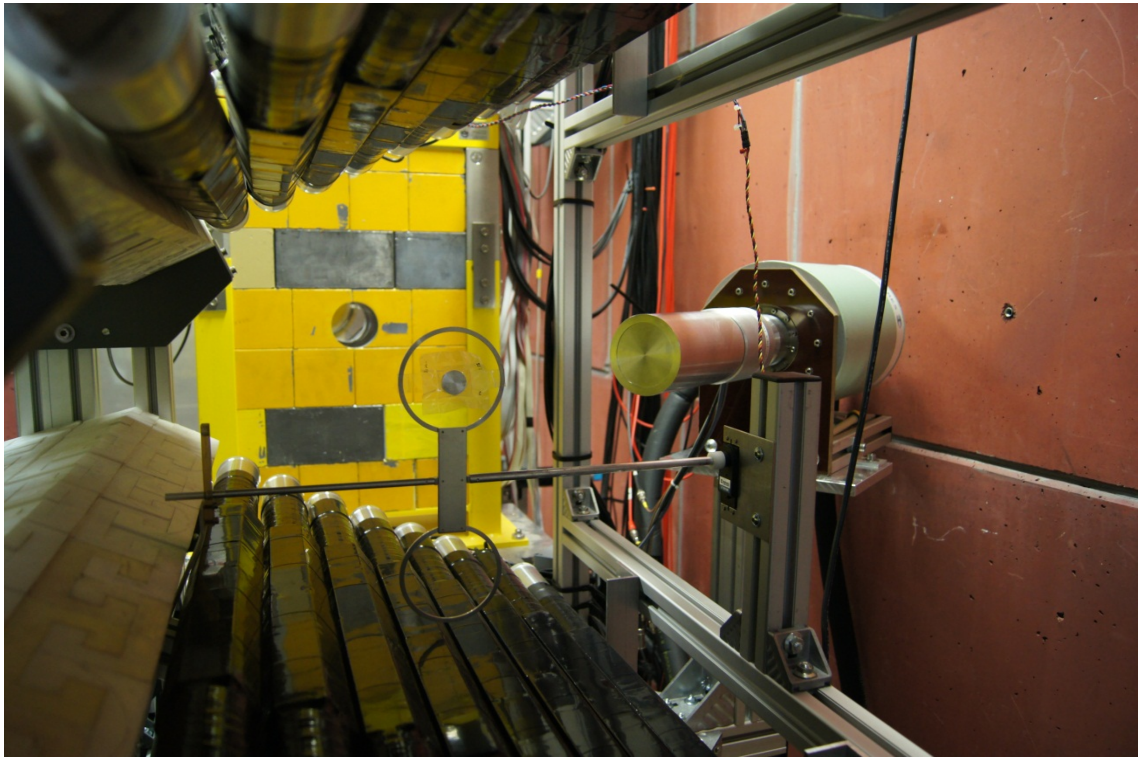

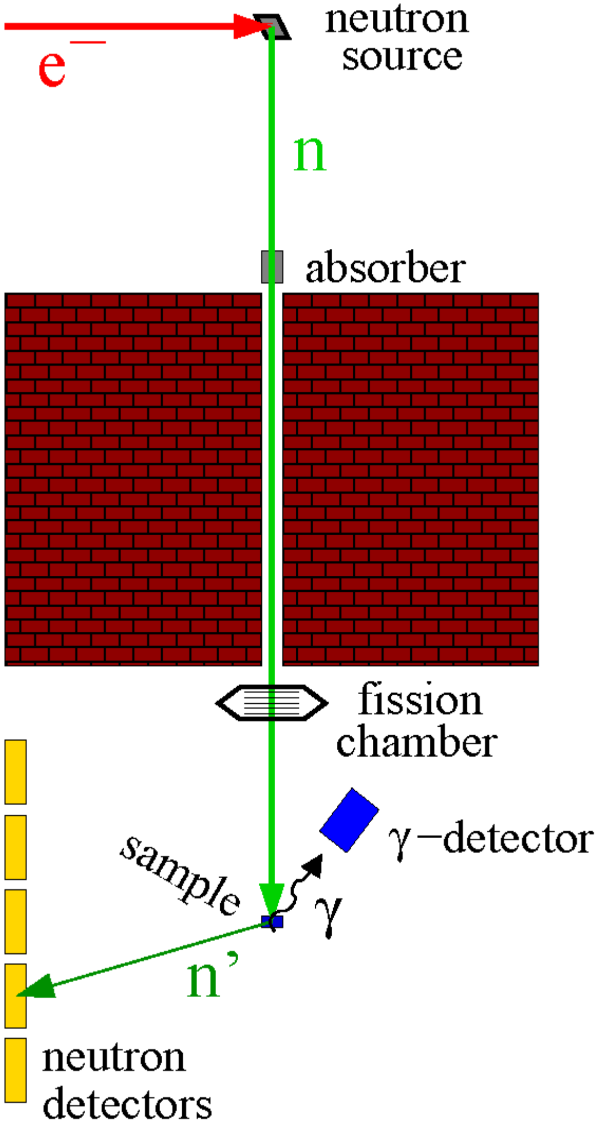

Target: cylinder of natural iron diameter 20 mm, thickness 8 mm

◦ HPGe detector at 125◦ to the neutron beam and a distance of 20 cm from the target

time-of-flight of the incident neutrons time resolution 10 ns

Measurements of photon production cross section

with target

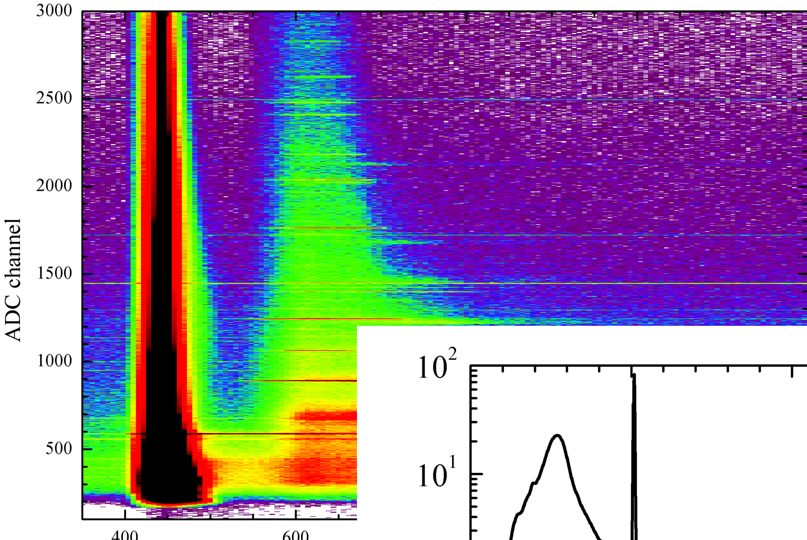

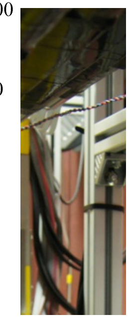

without target

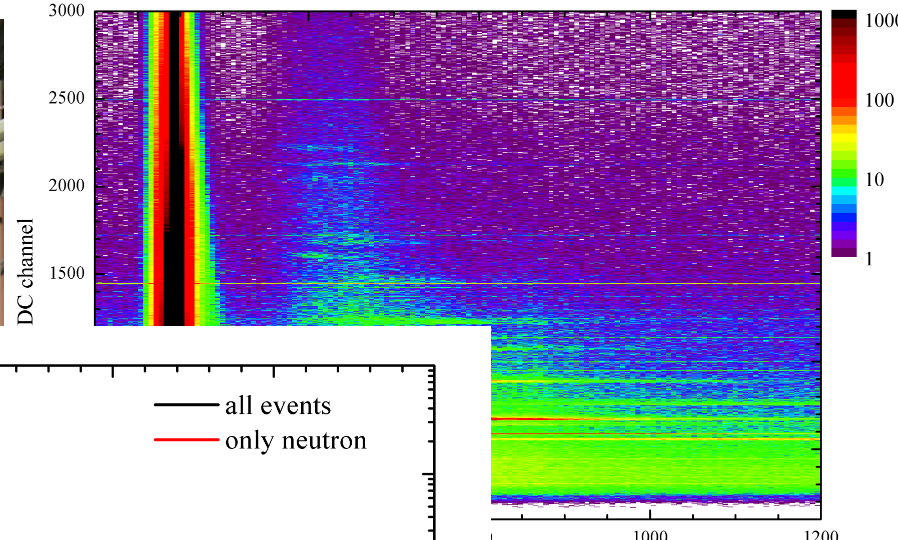

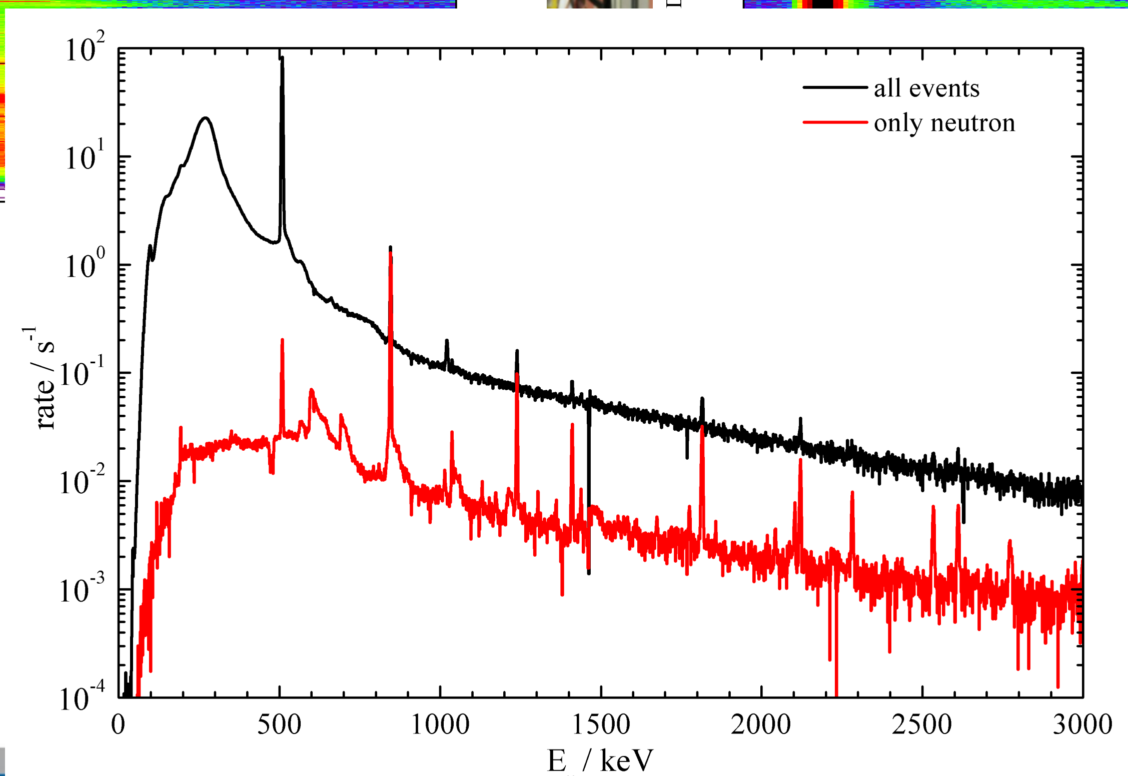

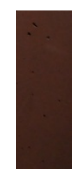

Time of flight Interval 11.72 ns

^{56}Fe decay scheme

Subtraction of feeding from higher lying states

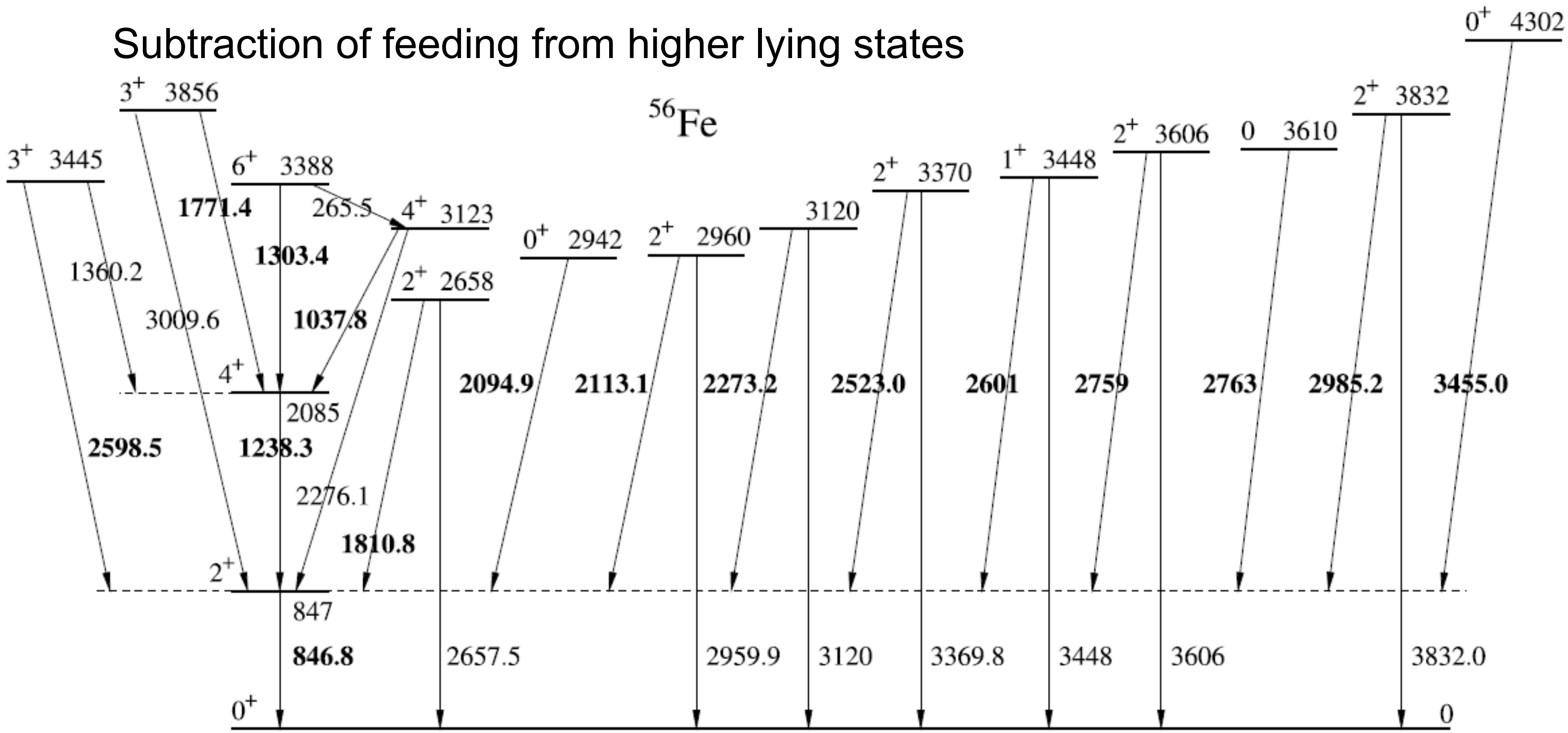

H. Junde, H. Su, and Y. Dong, Nucl. Data Sheets 112 (2011) 1513.

$$\sigma_{n',i}(E) = \sigma^p_{n',i}(E) - \sum_{j>i}^{E_x(L_j)\leqslant E} p(L_j \to L_i)\sigma^p_{n',j}(E)$$

Level cross section from level population cross sections

L.C. Michailescu et al. , NIM 531 (2004) 375

Feeding correction from measured transitions

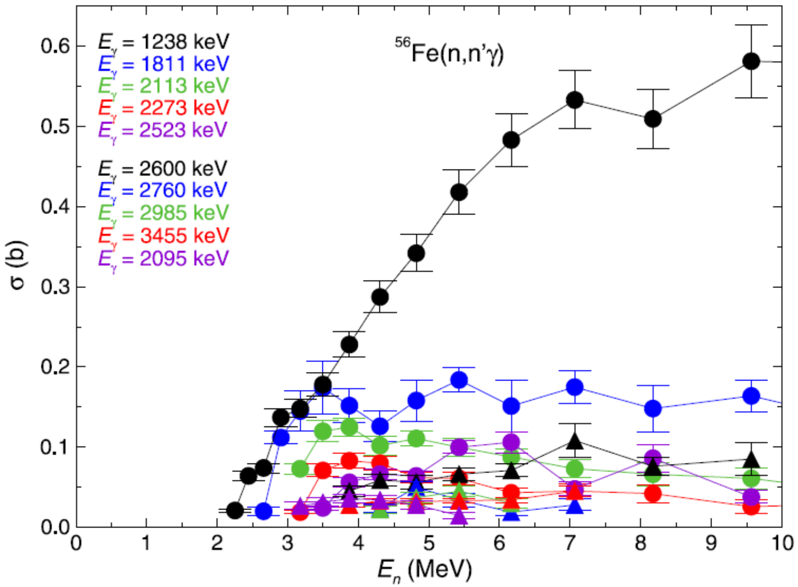

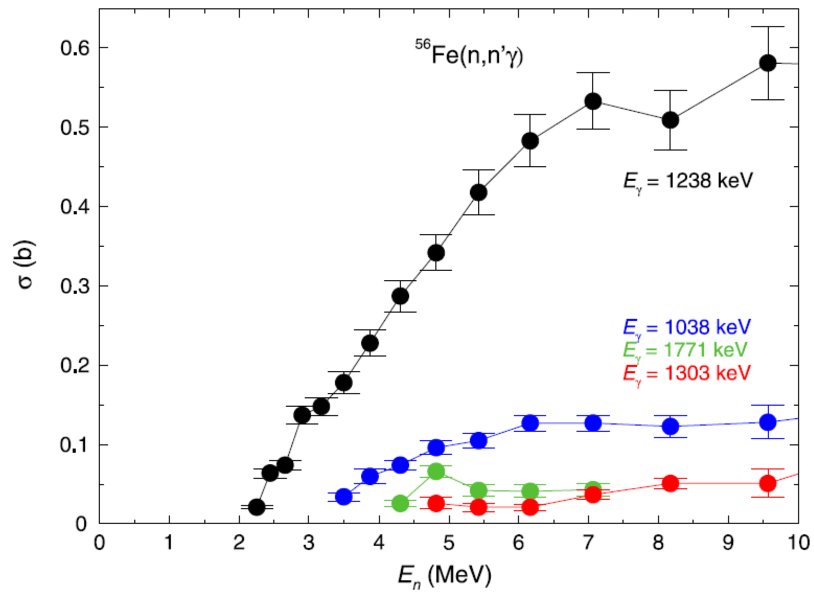

Gamma-ray production cross section of higher lying states feeding the 2_1^+ state (847 keV)

Gamma-ray production cross section of the 4_1^+ state (2085 keV) determined By the 1238 keV gamma ray and Feeding transitions from higher lying states

Method relies on a complete level scheme and gamma ray branching ratios

Corrections to the inelastic cross section

- Feeding from higher lying states
  (with observed gamma intensities)
- Probability of double scattering
  in the Fe sample 2% -10%
- Attenuation of the gamma rays in the Fe sample,
  e.g. 847 keV Factor 1.28
- Correction for angular distribution of emitted gamma-ray
  (4th order legendre polynomial) not applied

$$\frac{d\sigma}{d\omega}(E_n) = \frac{\sigma(E_n)}{4\pi}[1 + w_2(E_n)P_2(\cos\theta) + w_4(E_n)P_4(\cos\theta)]$$

Inelastic neutron scattering cross section on ^{56}Fe

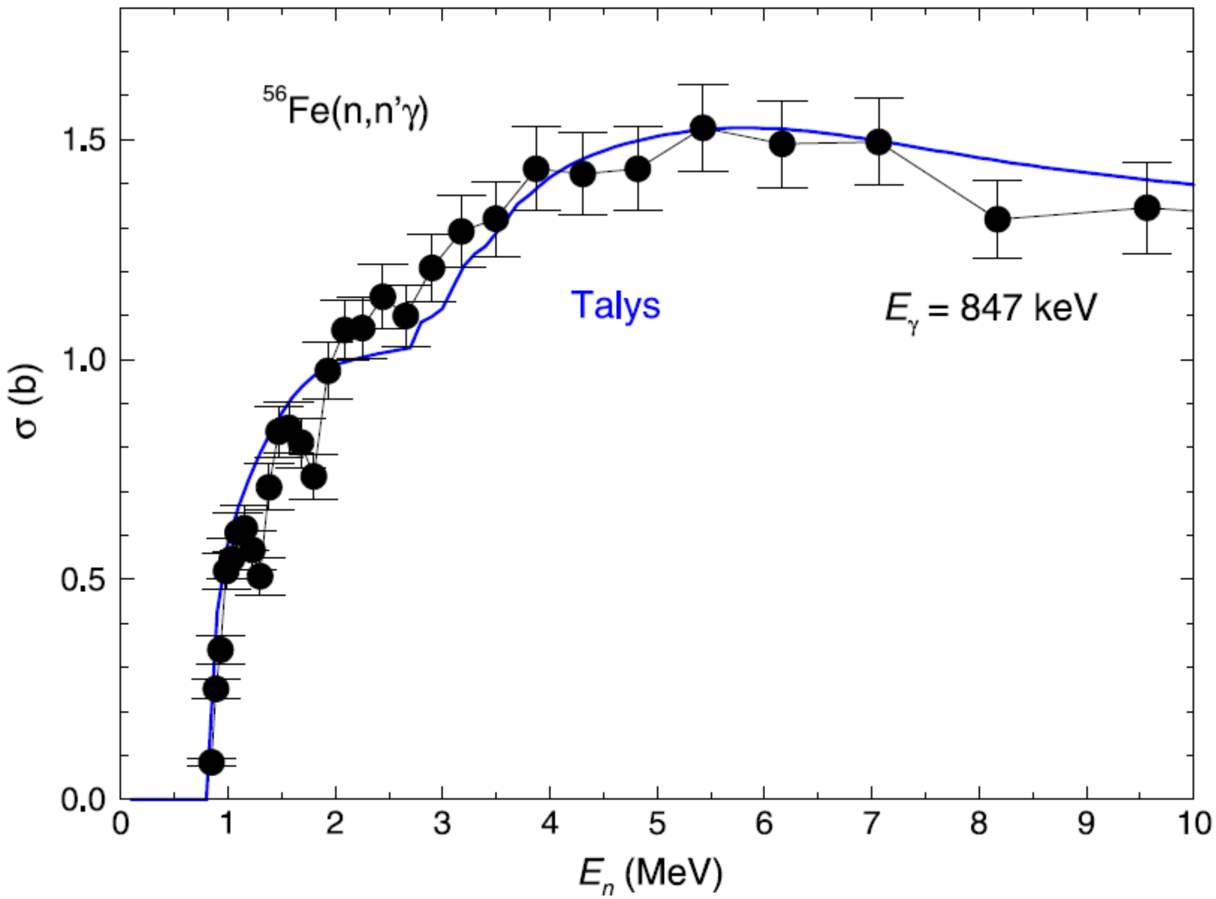

R. Beyer et al., Nuclear Physics A 927 (2014)

Inelastic scattering to the 1st excited state

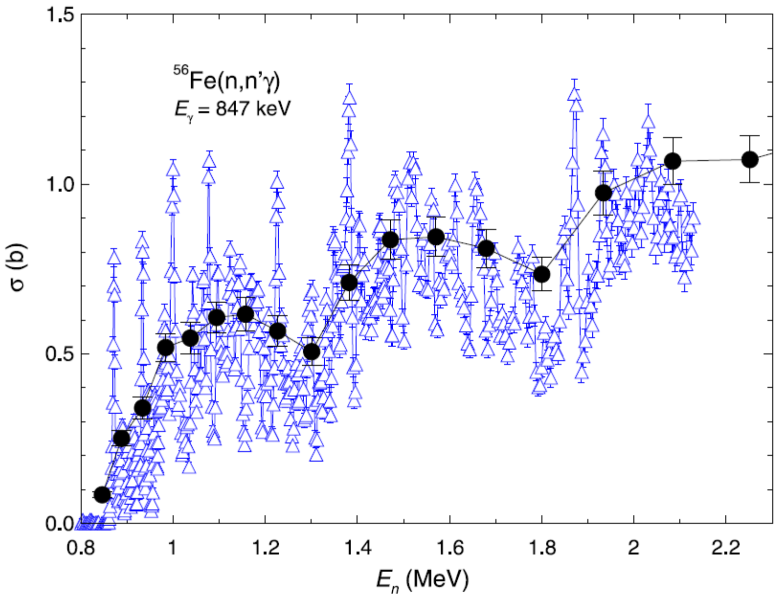

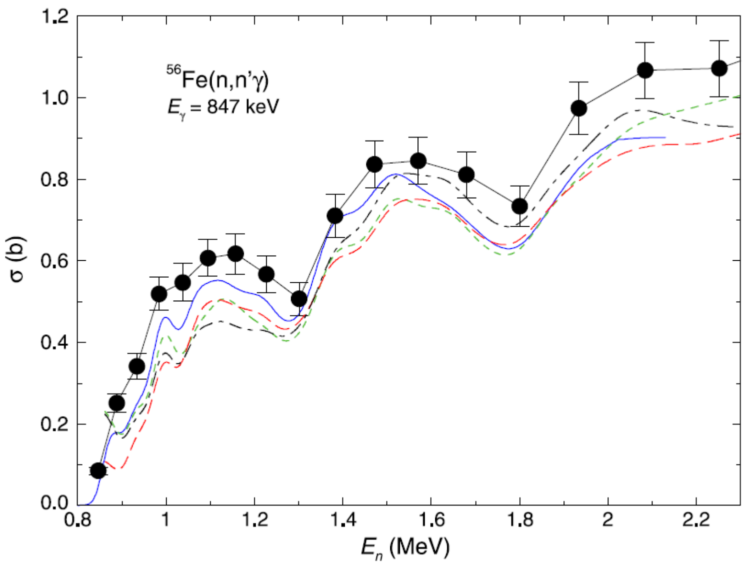

Perey et al. (1971) averaged

JEFF-3.1.

R. Beyer et al., Nuclear Physics A 927 (2014)

Inelastic scattering to the 2_1^+,4_1^+,6_1^+ states

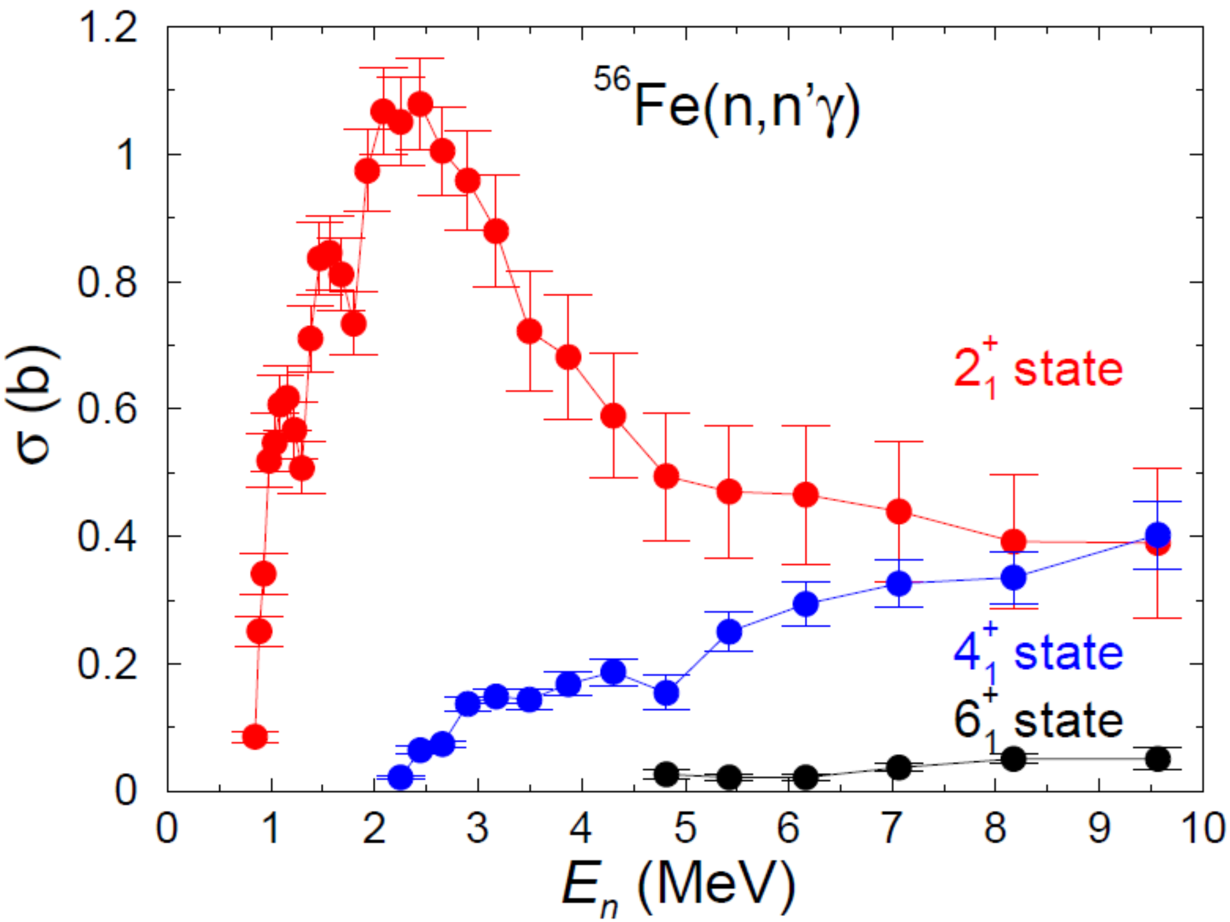

R. Beyer et al., Nuclear Physics A 927 (2014)

nELBE – double ToF detector setup

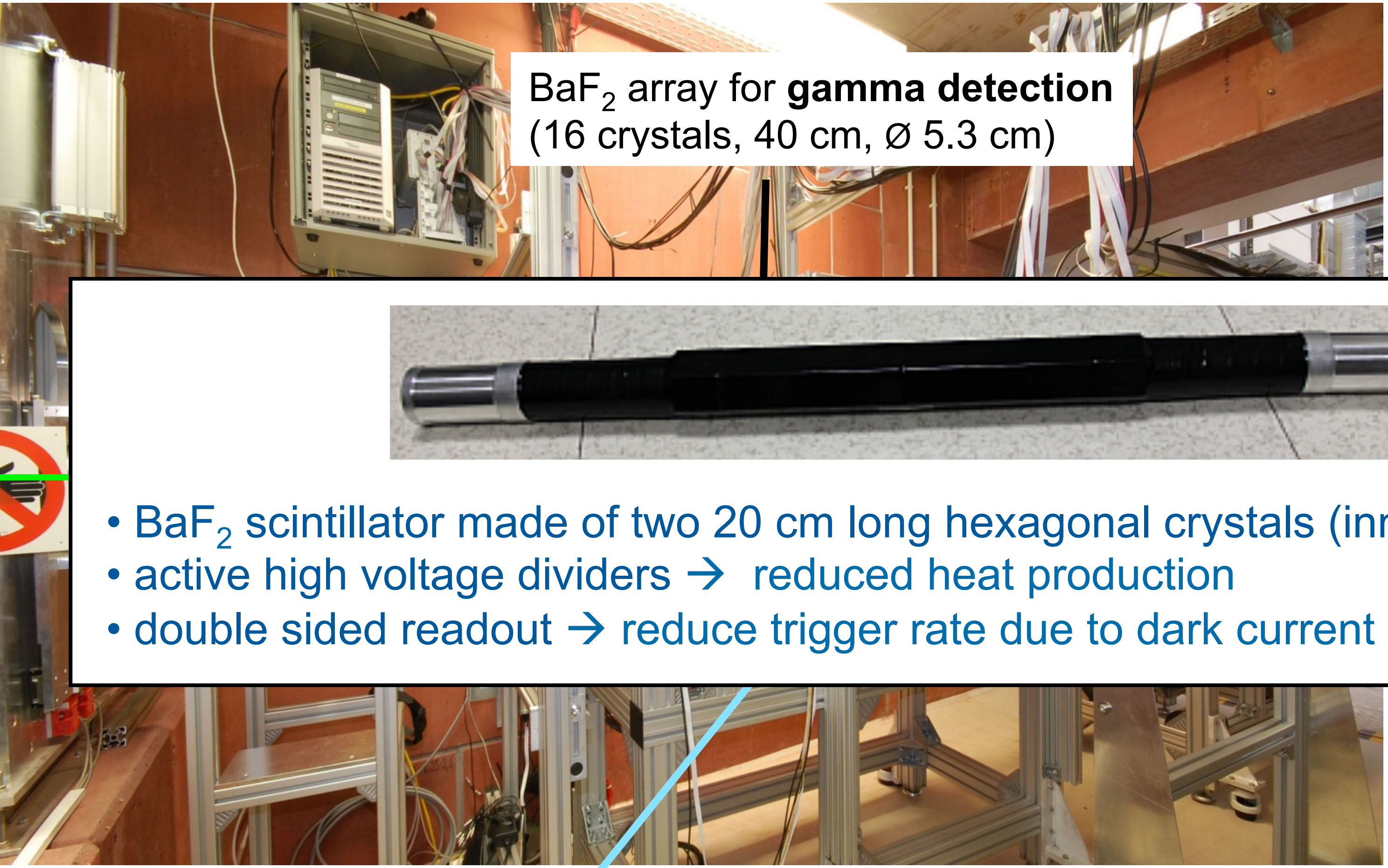

- BaF$_2$ scintillator made of two 20 cm long hexagonal crystals (inner Ø = 53 mm)
- active high voltage dividers → reduced heat production
- double sided readout → reduce trigger rate due to dark current

sample: ^{nat}**Fe** (99.8%) → 91.754% ^{56}Fe
mass: 19.82 g → 18.15 g ^{56}Fe

DRESDEN concept HZDR

nELBE – double ToF detector setup

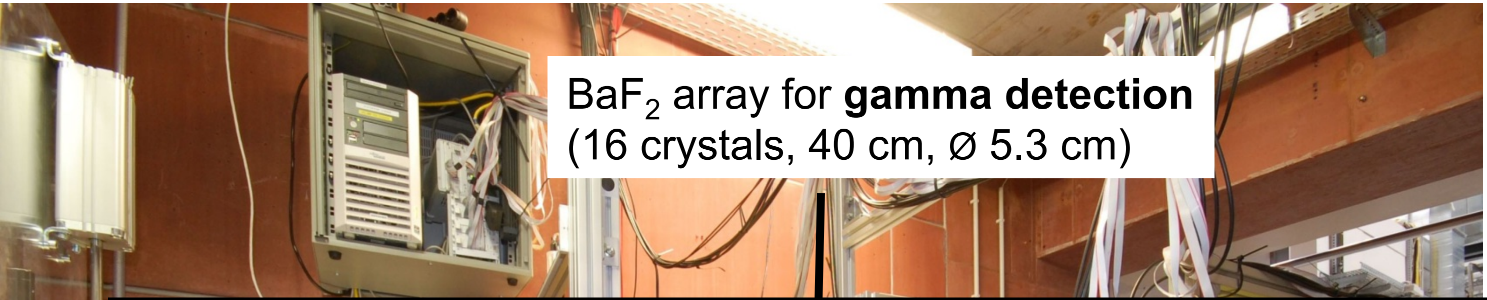

BaF$_2$ array for **gamma detection**
(16 crystals, 40 cm, ø 5.3 cm)

- EJ-200 plastic scintillator 1 m x 11 mm x 42 mm
- double sided readout → reduce trigger due to dark current
- active high voltage dividers → reduced heat production
- high gain photomultiplier + threshold just below single electron peak
  → neutron detection threshold approx. 20 keV
- surrounded by 1 cm Pb shielding to reduce background rate

sample: ^{nat}**Fe** (99.8%) → 91.754% ^{56}Fe
mass: 19.82 g → 18.15 g ^{56}Fe

DRESDEN concept

HZDR

nELBE – double ToF detector setup

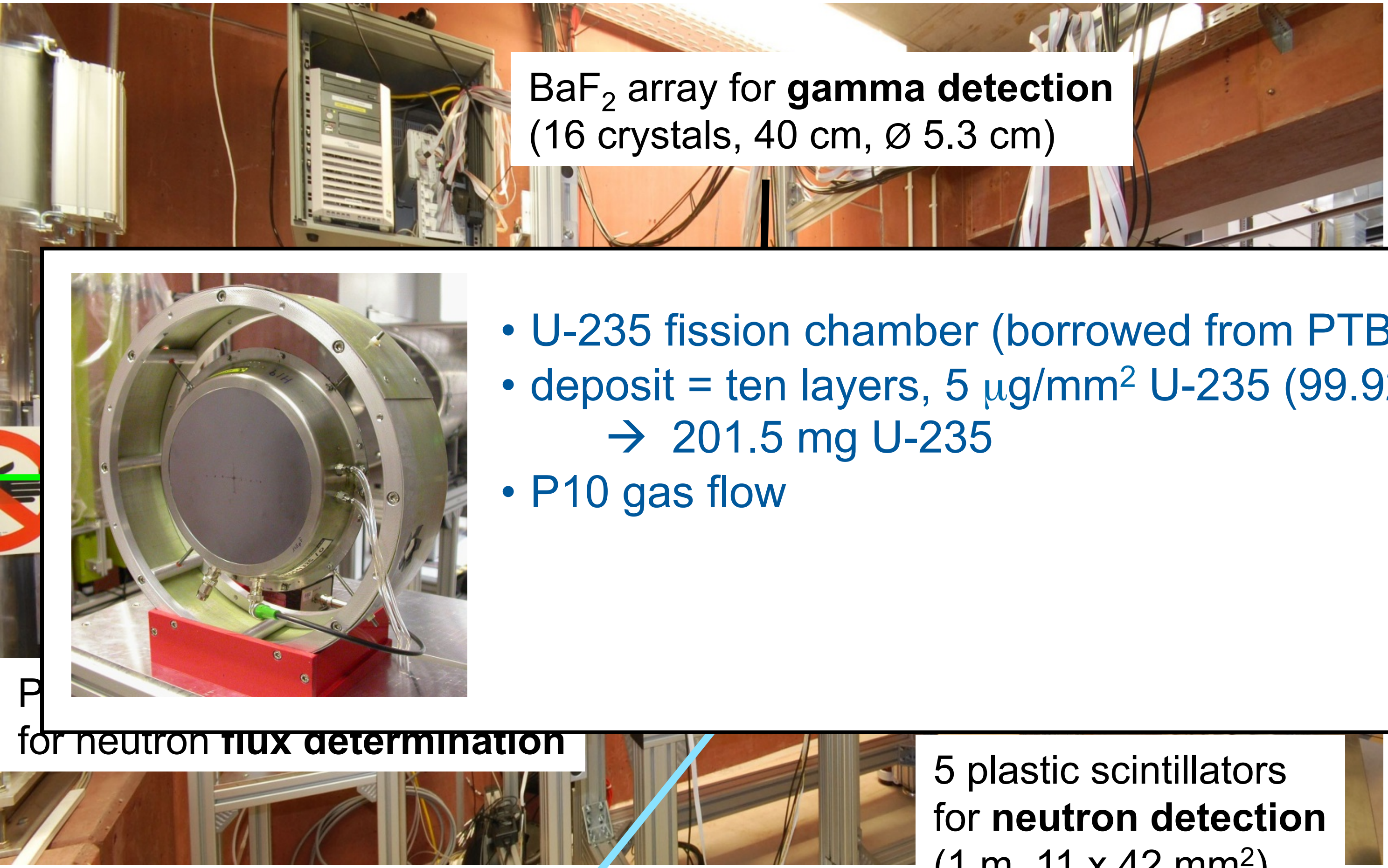

BaF_2 array for **gamma detection**
(16 crystals, 40 cm, Ø 5.3 cm)

flight paths:
source - FC:
400 cm
source - sample:

- U-235 fission chamber (borrowed from PTB Braunschweig)
- deposit = ten layers, 5 μg/mm² U-235 (99.92%), Ø 76mm
  → 201.5 mg U-235
- P10 gas flow

for neutron **flux determination**

5 plastic scintillators
for **neutron detection**
(1 m, 11 x 42 mm²)

sample: ^{nat}**Fe** (99.8%) → 91.754% ^{56}Fe
mass: 19.82 g → 18.15 g ^{56}Fe

DRESDEN concept HZDR

Detector geometry - details

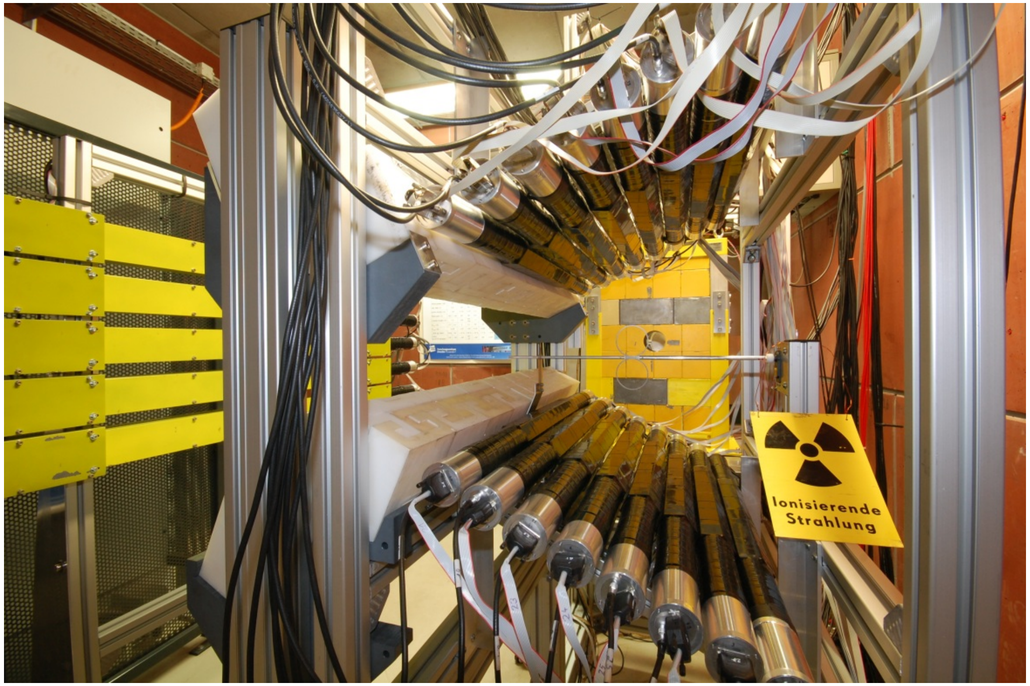

Plastics

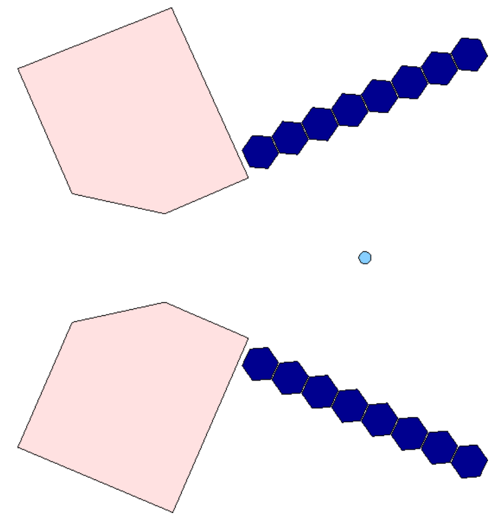

BaF_2-Setup

- ➔ borated polyethylene block between BaF_2 and plastics
- ➔ number of random coincidences reduced by one order of magnitude

angular coverage:

- θ_n = 60° - 120°
- θ_γ = 50° - 130°
- φ = +/- (30° - 130°)

Experimental method

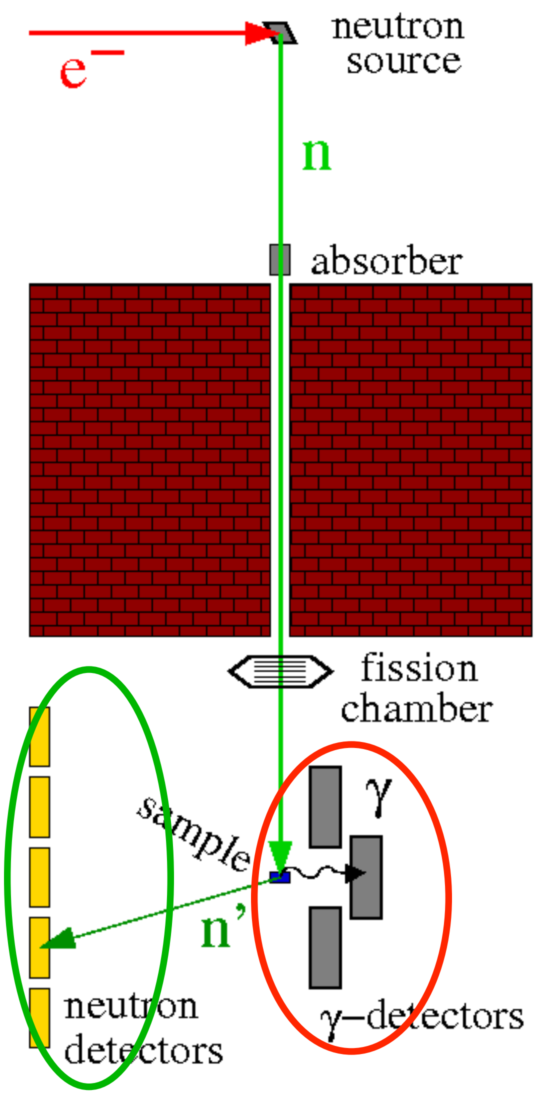

$$^{56}\mathrm{Fe}(n,n'\gamma)^{56}\mathrm{Fe}\ \begin{cases} ^{56}\mathrm{Fe}+n \rightarrow {}^{56}\mathrm{Fe}^{*} + n' \\ ^{56}\mathrm{Fe}^{*} \rightarrow {}^{56}\mathrm{Fe} + \gamma \end{cases}$$

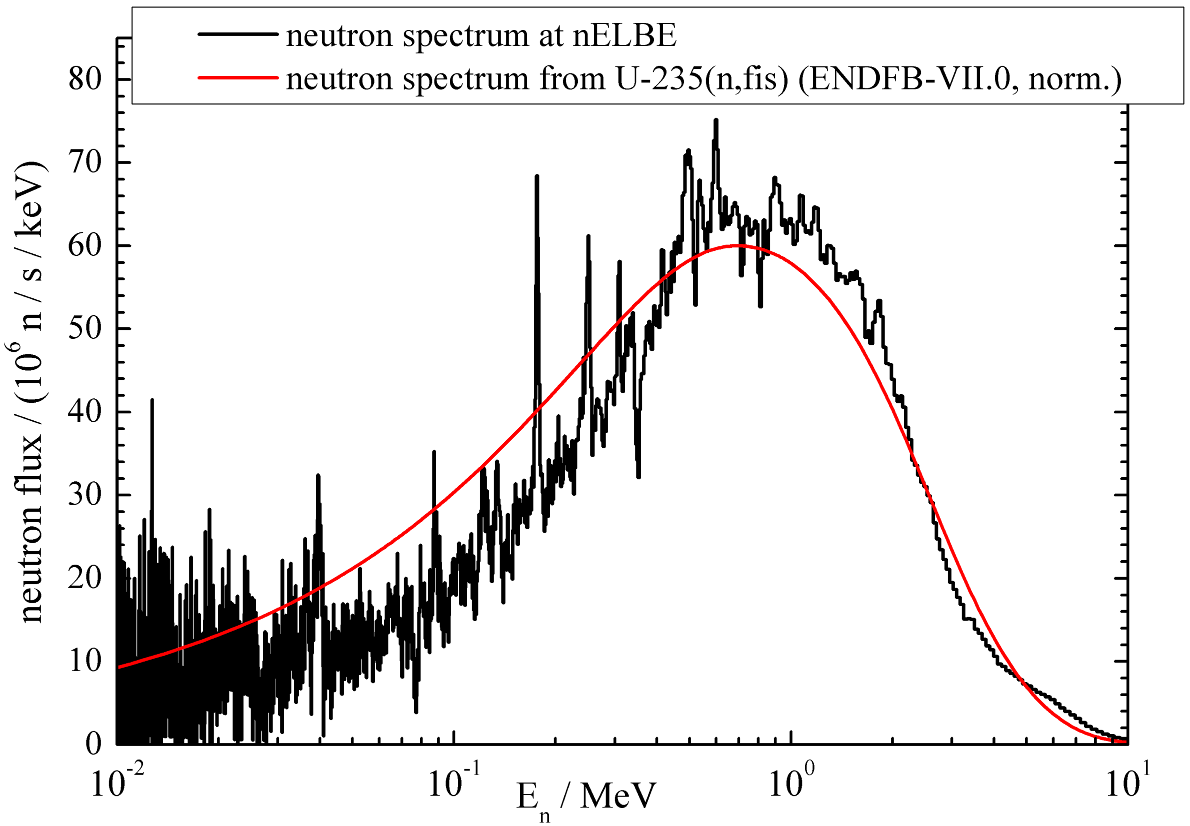

Experimental method

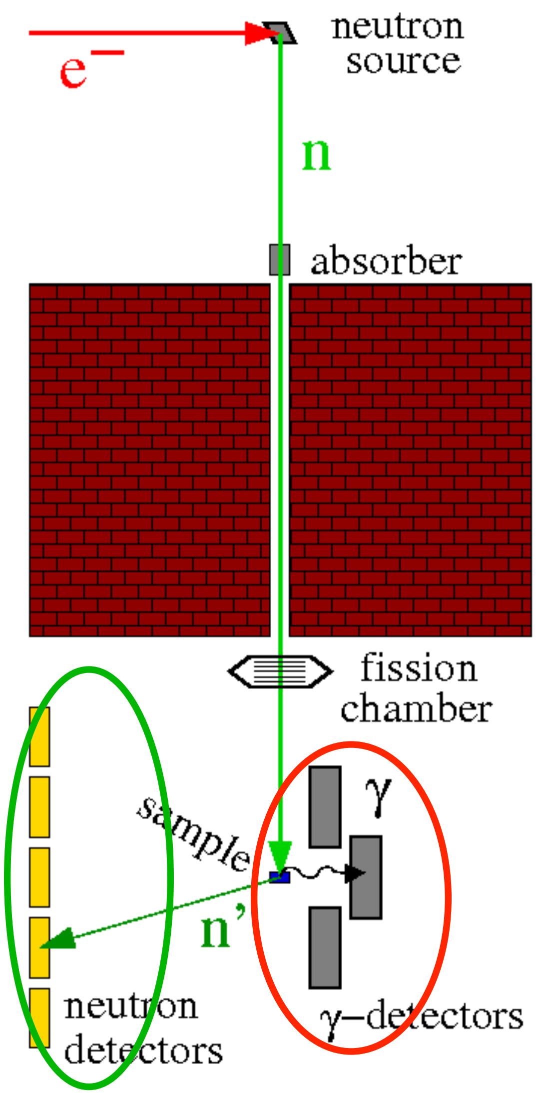

$$^{56}Fe(n,n'\gamma)^{56}Fe \begin{cases} ^{56}Fe + n \rightarrow {}^{56}Fe^* + n' \\ \qquad ^{56}Fe^* \rightarrow {}^{56}Fe + \gamma \end{cases}$$

without sample (82 h live time)

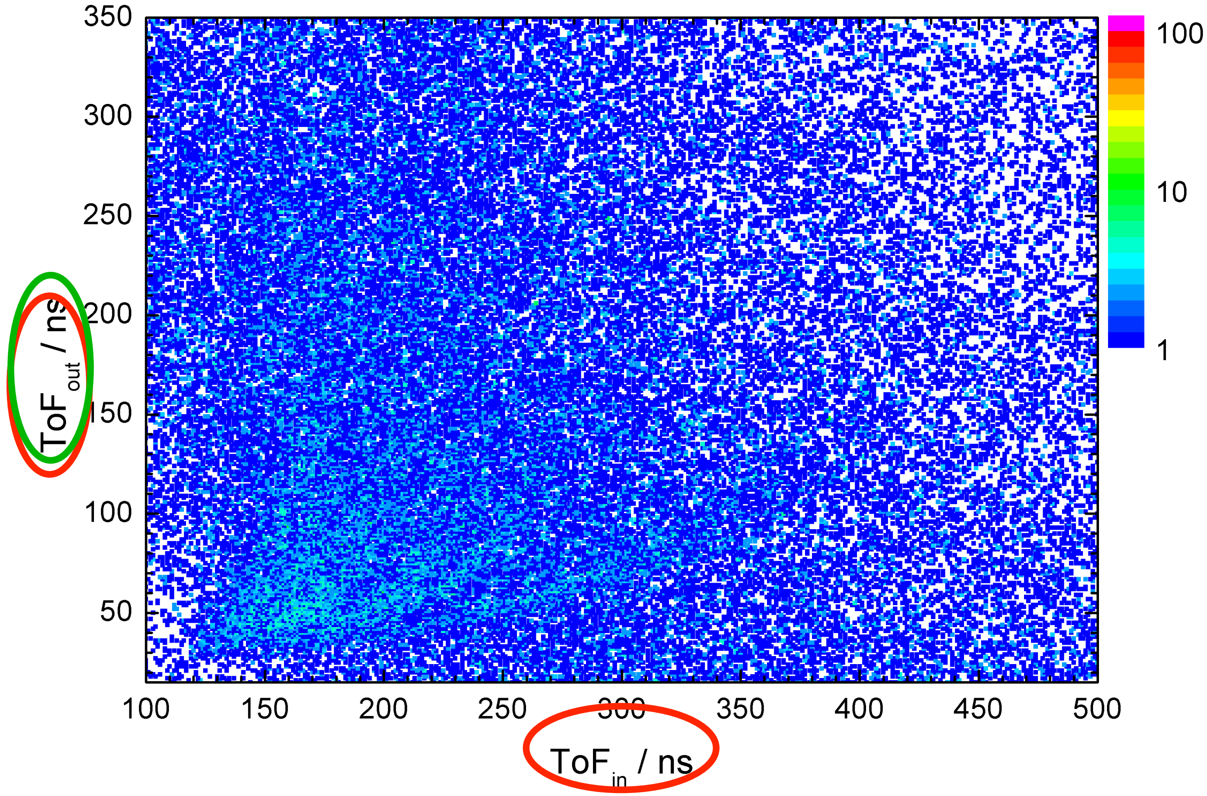

Experimental method

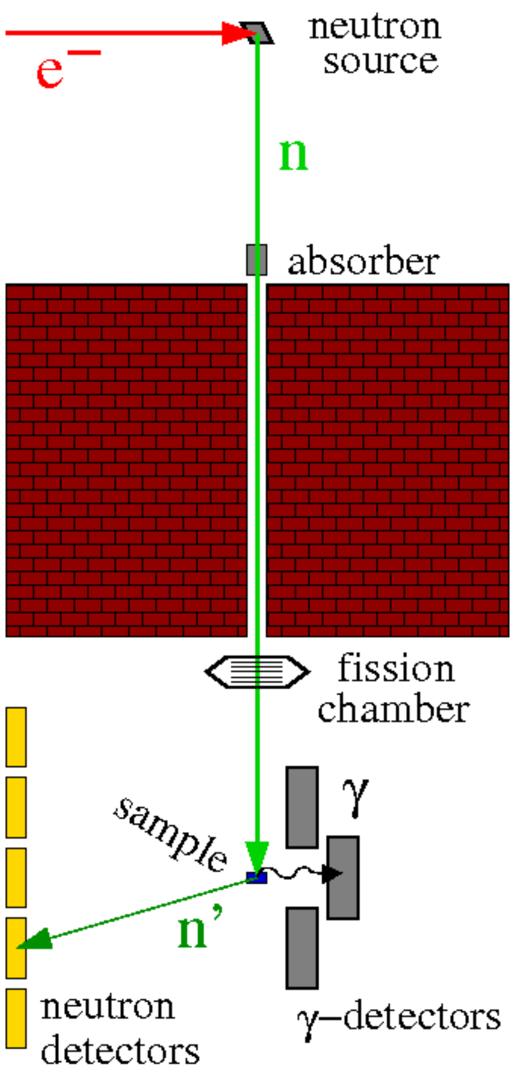

$$^{56}Fe(n,n'\gamma)^{56}Fe \left\{ \begin{array}{l} ^{56}Fe + n \rightarrow {}^{56}Fe^{*} + n' \\ ^{56}Fe^{*} \rightarrow {}^{56}Fe + \gamma \end{array} \right.$$

with sample (78 h live time)

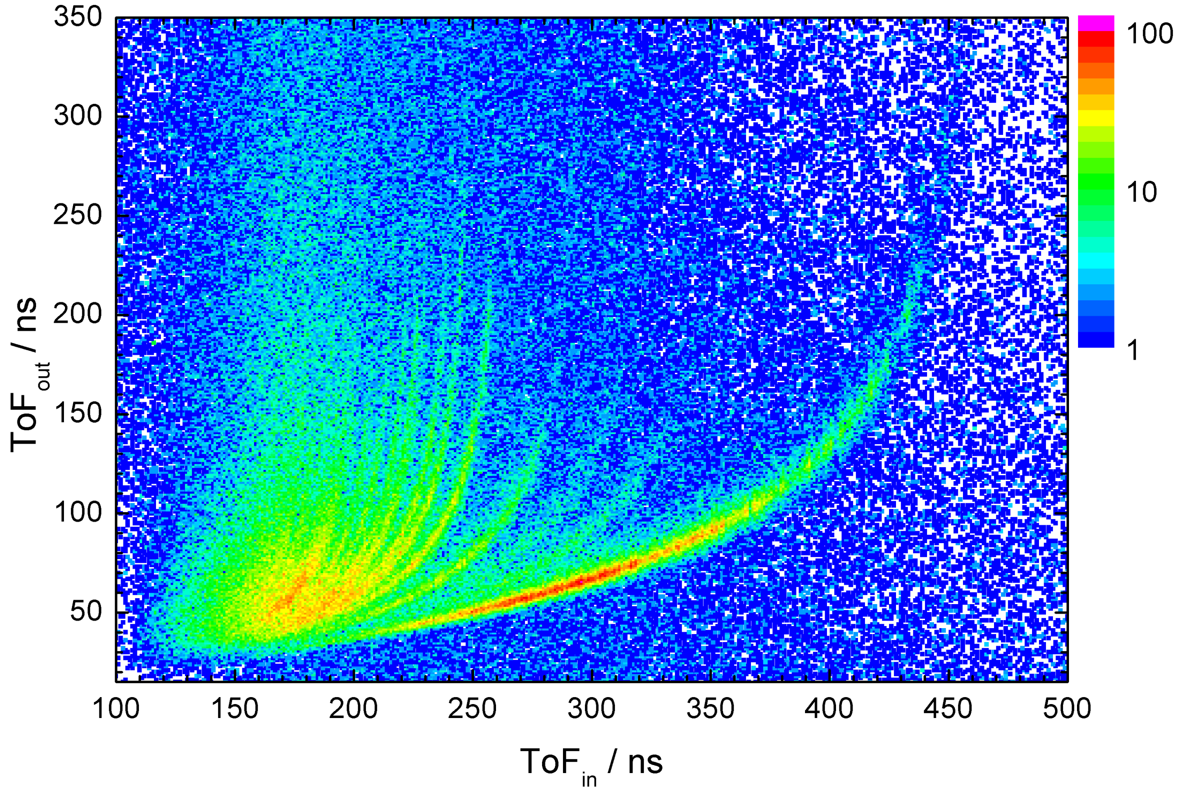

Kinematic calculations

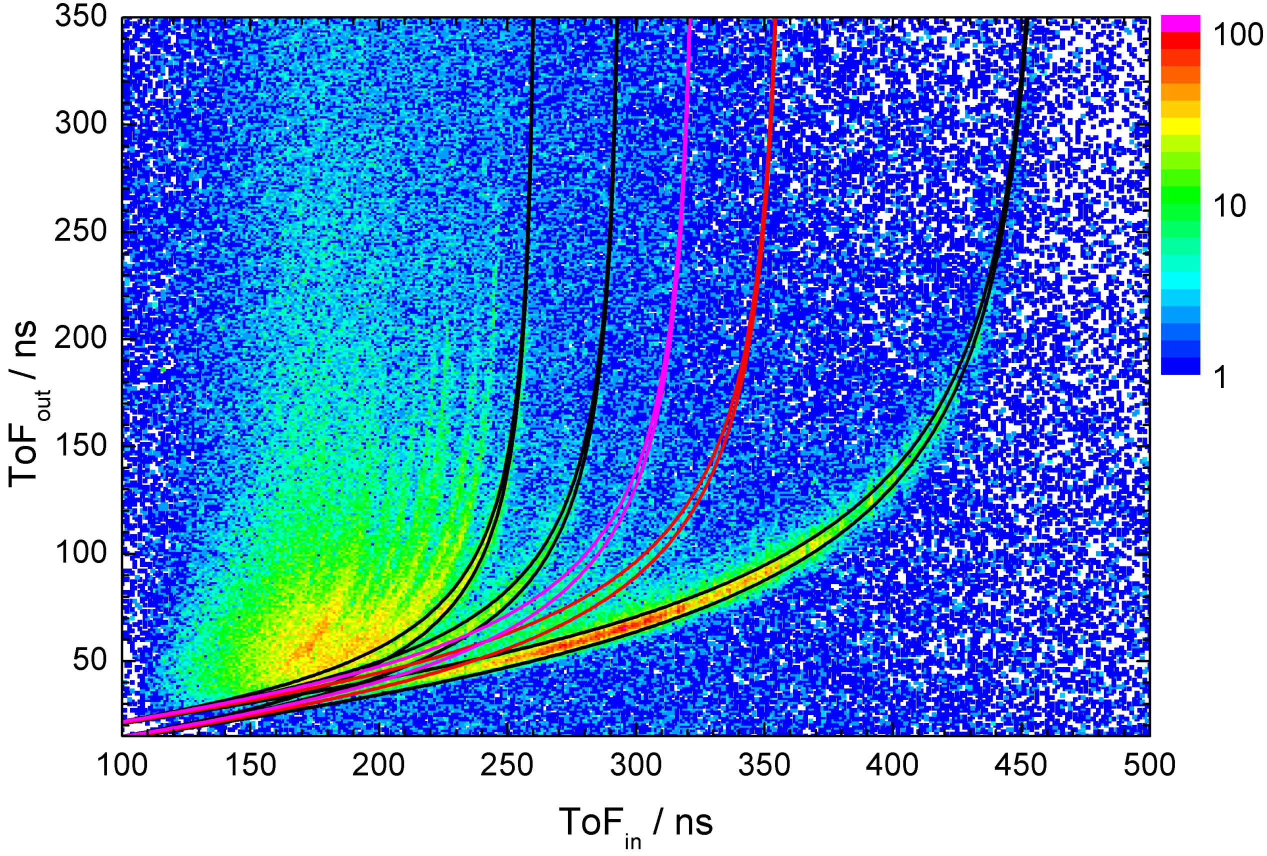

-Fe-56 (1.,2.,3. Level)
(847, 2085, 2658 keV)

-Fe-54 (1. Level)
(1408 keV)

-Fe-56 (2 x 1. Level)
(1694 keV)

The $^{56}Fe(n,n'\gamma)$ cross section for the 1st excited state

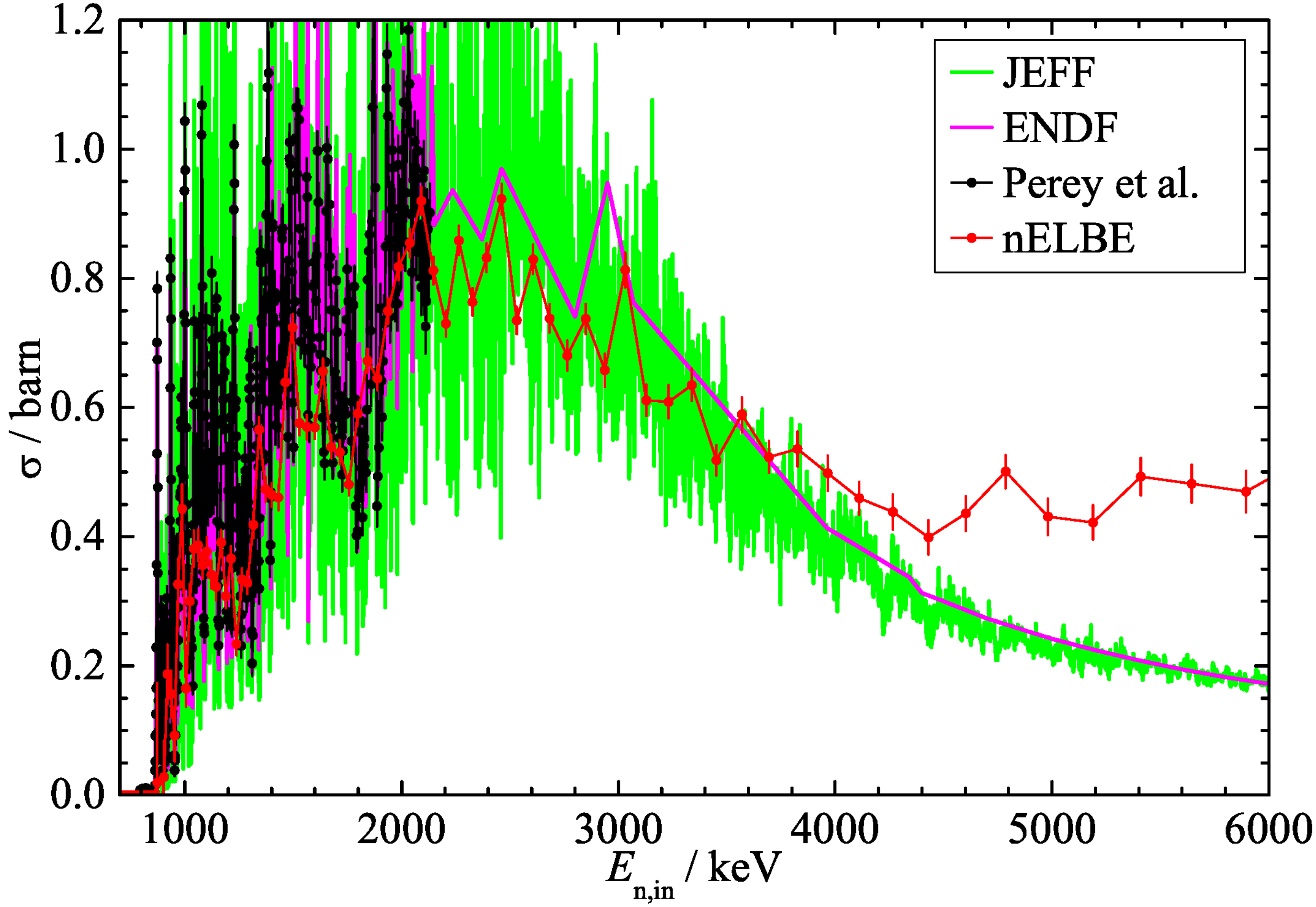

DRESDEN concept HZDR

The $^{56}Fe(n,n'\gamma)$ cross section for the 1st excited state

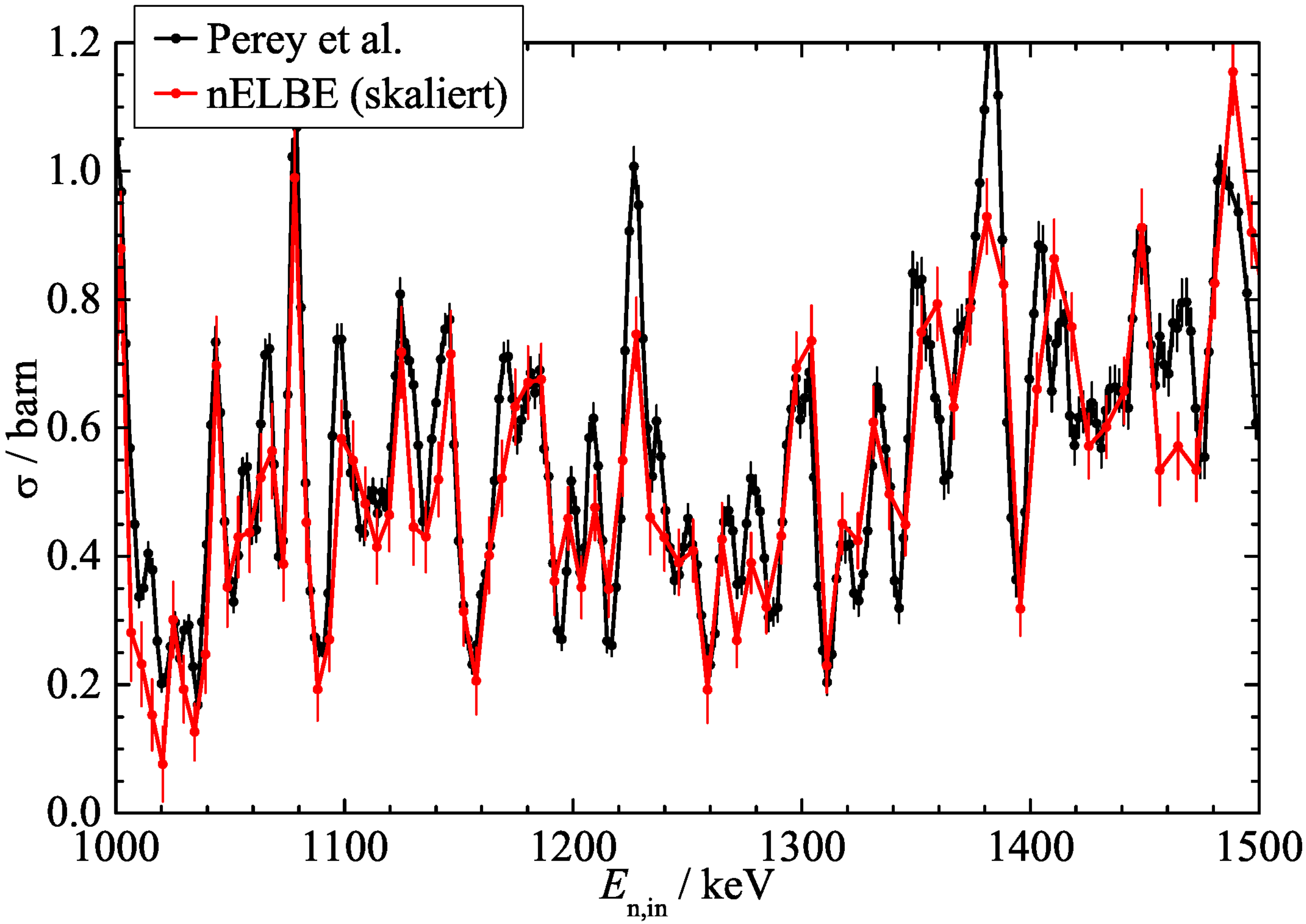

The ^{56}Fe(n,n'γ) cross section for the 1st excited state

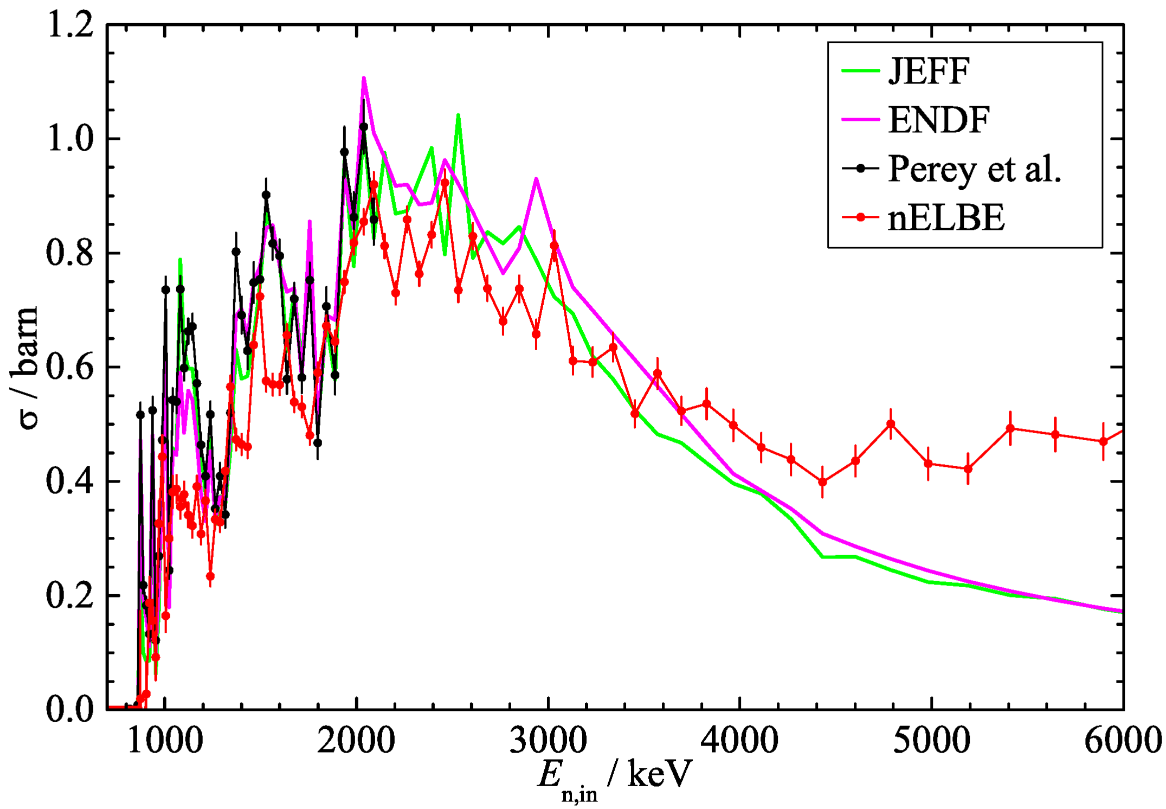

<u>Corrections included</u>

- Fission chamber efficiency
- Fission chamber random background
- Loss due to ADC range
- Flux attenuation in fission chamber
- Flux attenuation in air
- Flux attenuation in target
- Beam diameter at target position
- Target diameter
- Gamma absorption in target

- 2D-ToF background
- BaF2 efficiency
- plastic efficiency

JEFF, ENDF resolution averaged to experimental resolution
nELBE double time of flight data systematically lower
Possible angular correlation between n‘ and γ not observable due to
Low counting statistics in the individual detector pairs.

DRESDEN concept HZDR

Angular correlation of γ and n‘

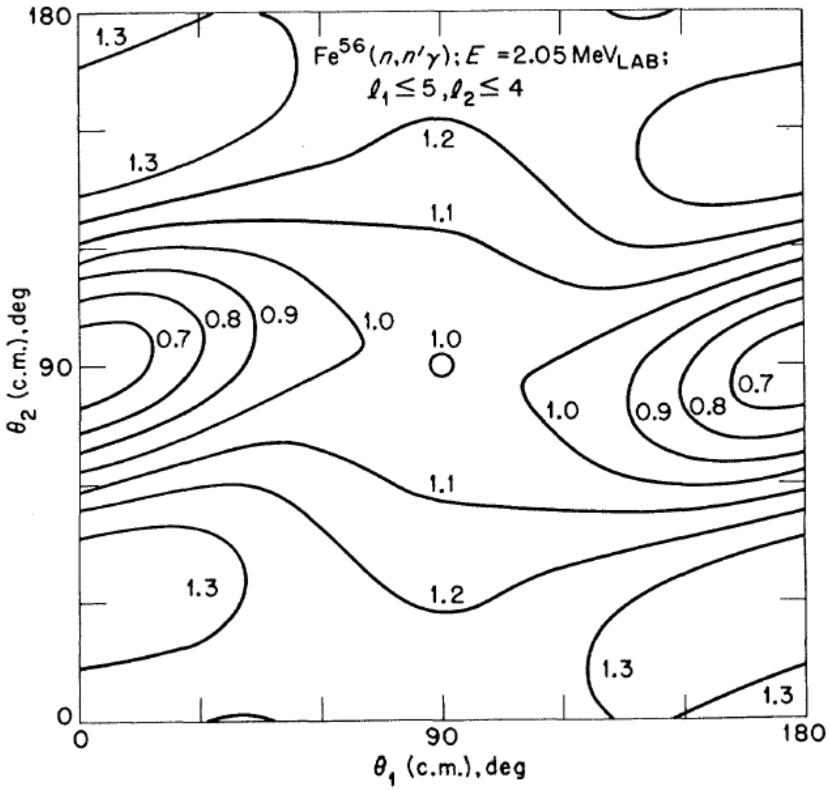

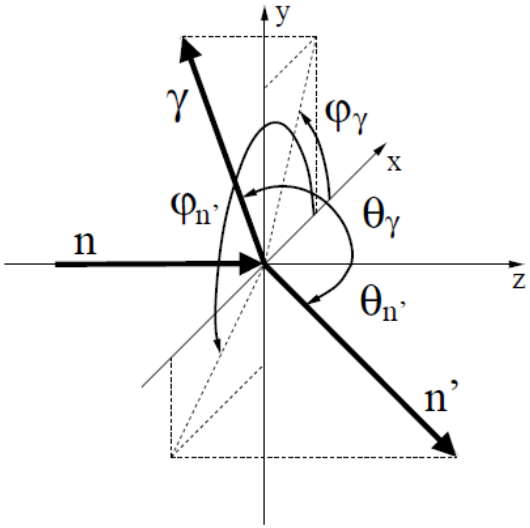

Statistical Model of nuclear reactions ➔
Angular correlation of the emitted γ and the scattered neutron:

R. Beyer Dissertation 2014, E. Sheldon, Rev. Mod.Phys. 35 (1963) 795

Angular correlation measurement $^{56}Fe(n,n'\gamma)$

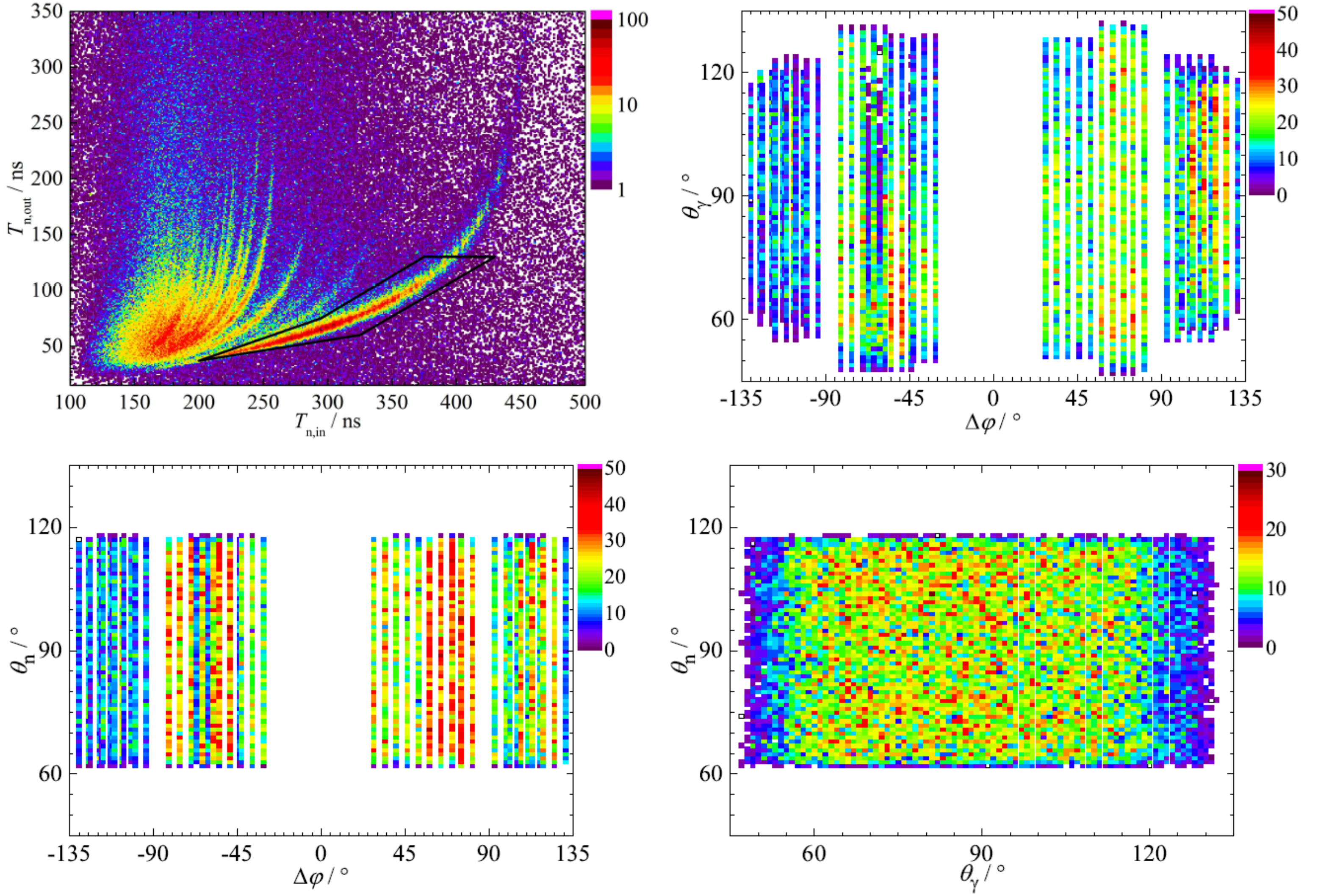

Counting statistics is insufficient to observe the angular correlation

Angular distribution setup

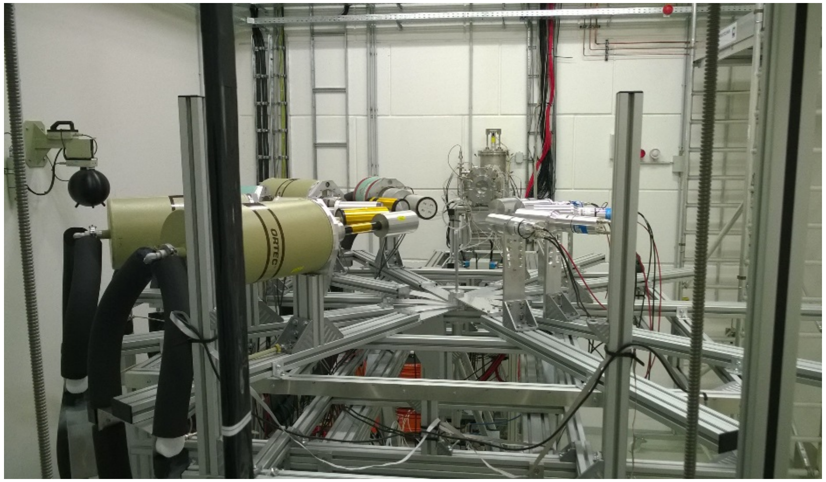

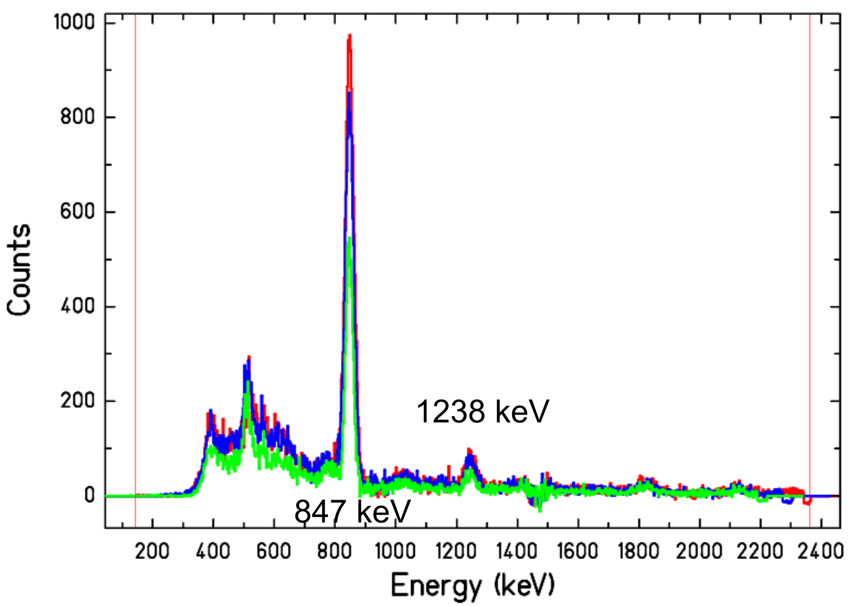

Time of flight vs. energy (uncalibrated)

Study (n,n'γ) angular distribution and cross sections with HPGe and $LaBr_3$

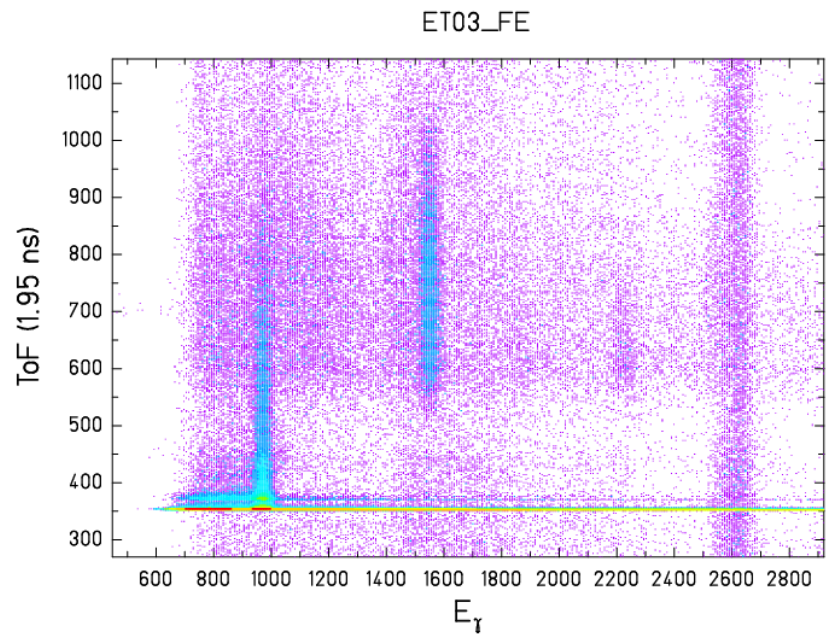

$LaBr_3$ Energy spectrum
(Target out background subtracted + Time of flight gate for neutrons)

DRESDEN concept HZDR

Inelastic scattering

Neutron time-of-flight with digital processing

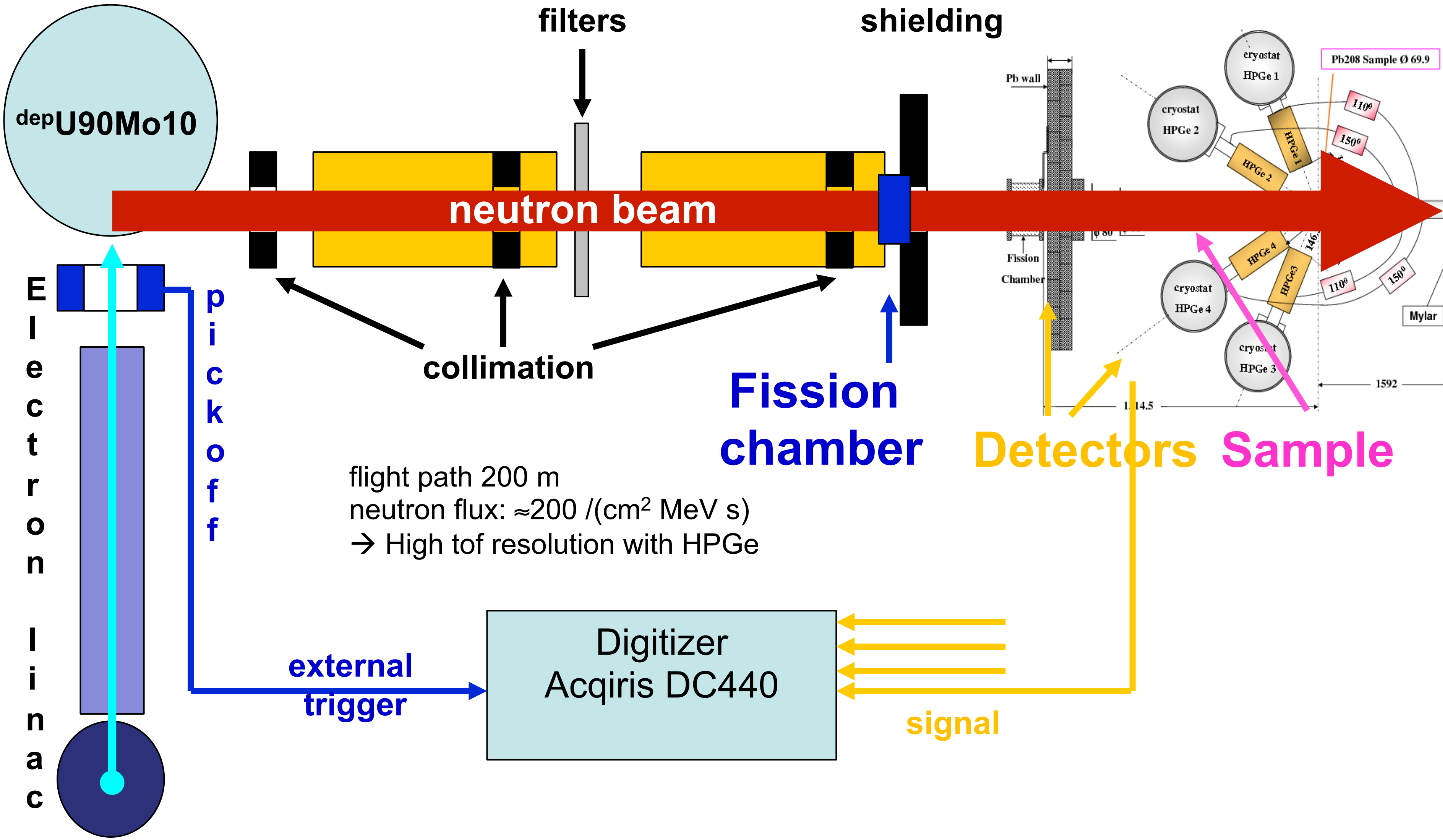

Courtesy: Arjan Plompen

GAINS Experiment at GELINA

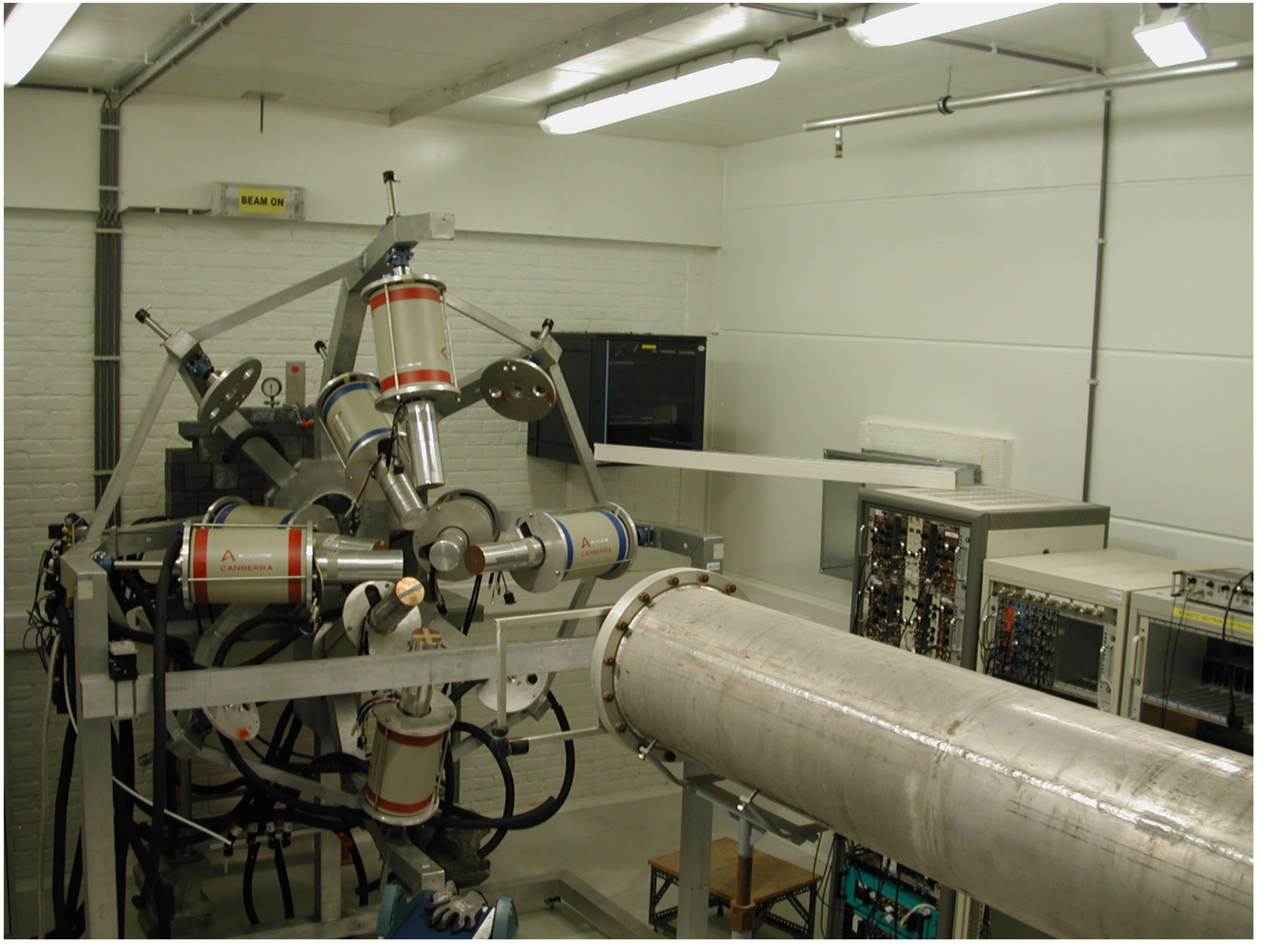

8 HPGe detectors under angles 110° and 150° to the beam,
^{235}U FC for neutron fluence determination
Sample e.g. ^{nat}Fe thickness 3 mm, diameter 80 mm

Integral production cross section of 847 keV γ rays in ^{56}Fe

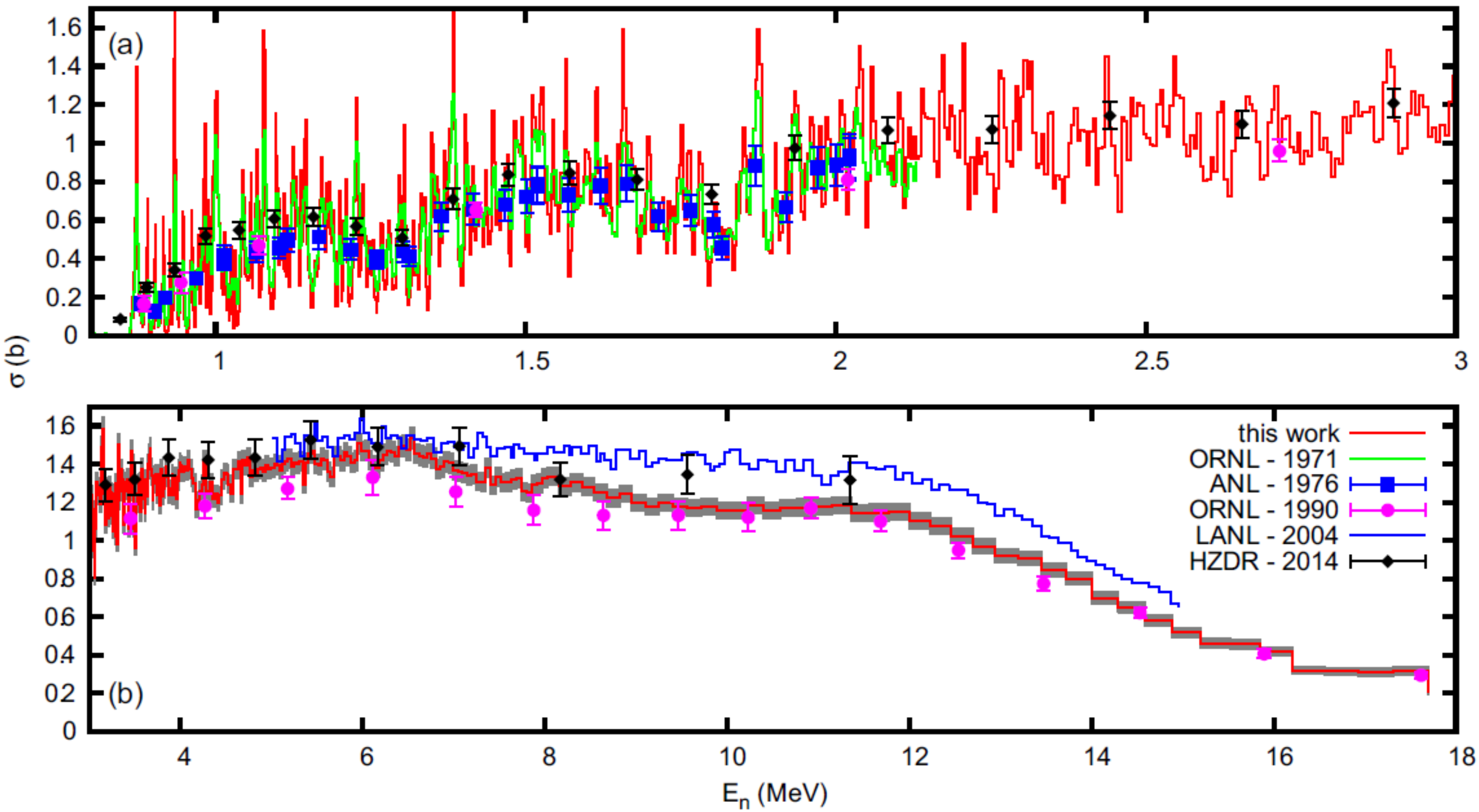

Collects most of the inelastic strength. → total inelastic cross section

A. Negret et al. Phys. Rev. C 90 (2014) 034602

Level cross sections for $^{56}Fe(n,n'\gamma)$

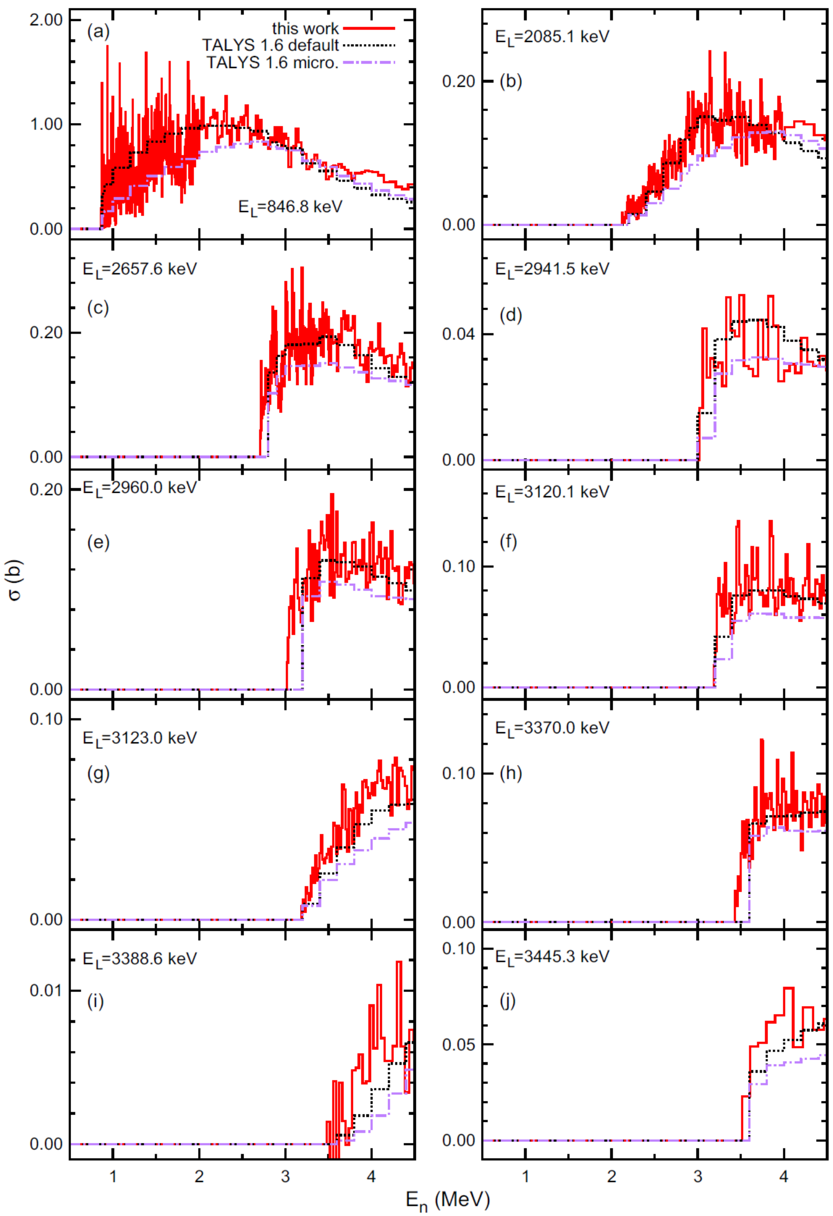

A. Negret et al. Phys. Rev. C 90 (2014) 034602

Comparison with evaluated data

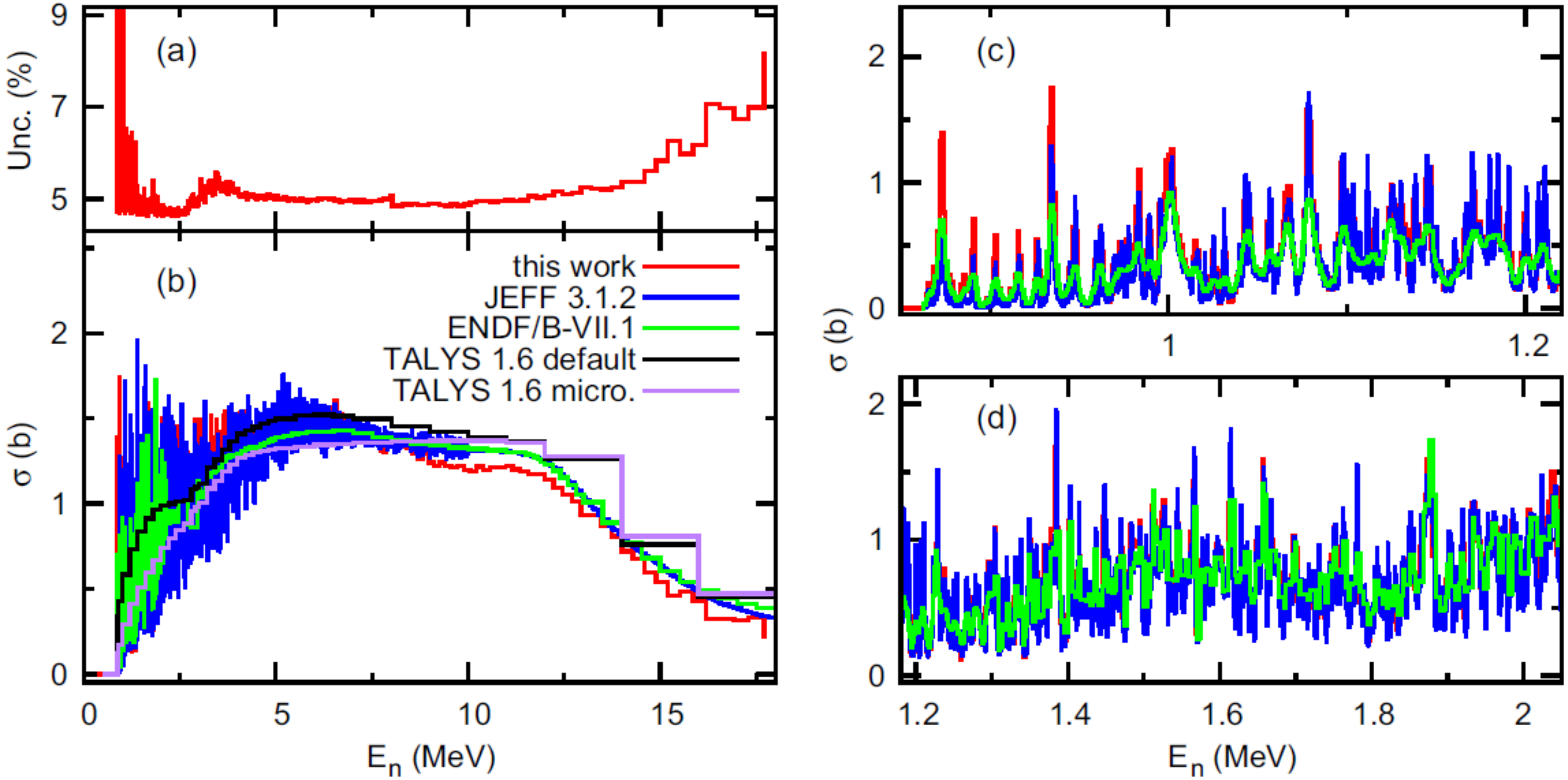

At the first few hundred keV the resonant structure might correspond to single resonances
Of the compound nucleus $^{57}Fe^*$
At higher energies the density of resonances is much smaller than expected from the level density models → Ericson fluctuations
A. Negret et al. Phys. Rev. C 90 (2014) 034602

Neutron inelastic scattering $^{22}Na(n,n',\gamma)$ measured at GAINS

92 C. Rouki et al. / Nuclear Instruments and Methods in Physics Research A 672 (2012) 82–93

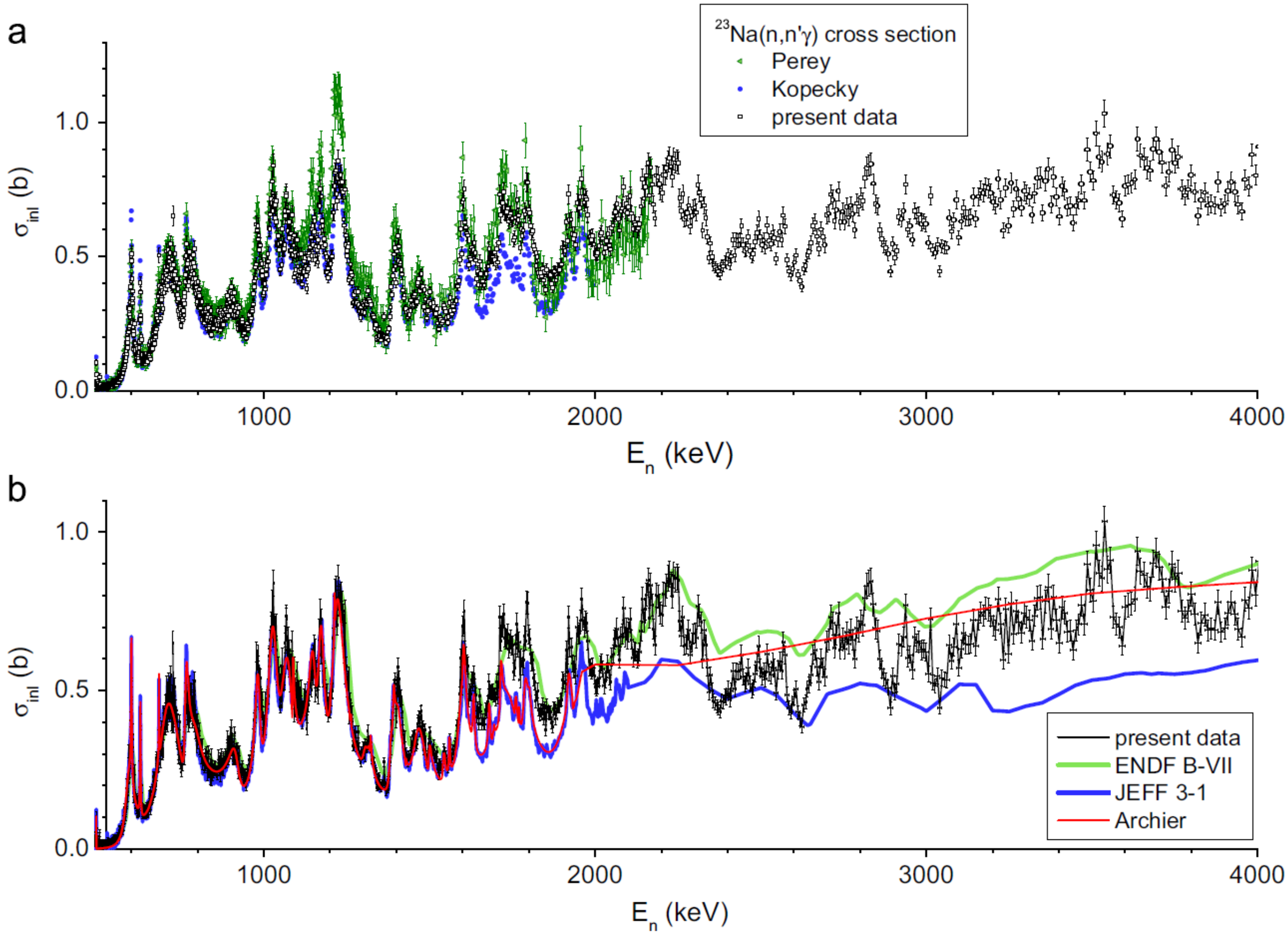

Fig. 10. The measured total inelastic cross-section for ^{23}Na (a) compared with earlier measurements and (b) with evaluated data from Archier [42] and the ENDF B-VII [41]and JEFF 3.1 [40] libraries.

C. Rouki et al., NIM A672 (2012) 82

^{26}Al(n,p) ^{26}Al(n,α) time of flight measurement at GELINA

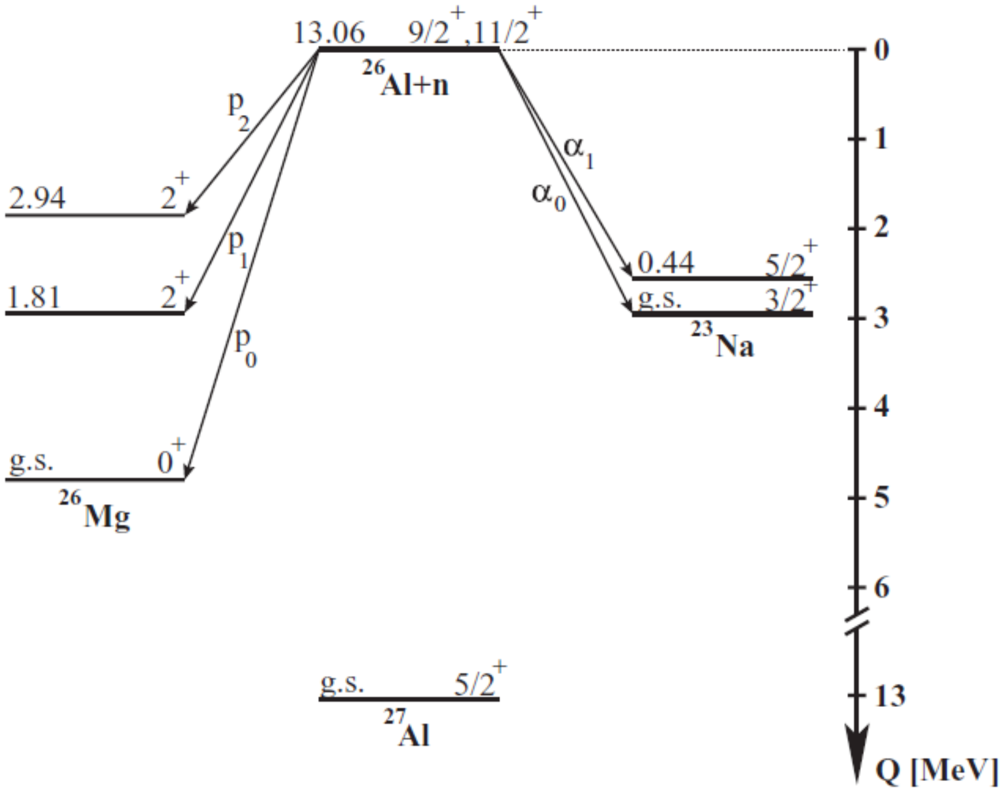

FIG. 2. Level scheme for the ^{26}Al(n, α_i)^{23}Na and ^{26}Al(n, p_i)^{26}Mg reactions. The energies are given in MeV.

- ^{26}Al sample 6*5 cm^2 $(2.58 \pm 0.12)\ 10↑17$ atoms (very little target material !!!)
- Time of flight measurement at GELINA flight path 8.45 m
- Frisch gridded ionisation chamber to detect n,α
- Neutron intensity from separate measurement of ^{10}B(n, α) reference deposit in FGIC

$$\sigma_{^{26}\mathrm{Al}}(E_n) = \frac{\epsilon_{^{10}\mathrm{B}}}{\epsilon_{^{26}\mathrm{Al}}} \frac{Y_{^{26}\mathrm{Al}}(E_n) - Y^{\mathrm{BG}}_{^{26}\mathrm{Al}}(E_n)}{Y_{^{10}\mathrm{B}}(E_n) - Y^{\mathrm{BG}}_{^{10}\mathrm{B}}(E_n)} \frac{N_{^{10}\mathrm{B}}}{N_{^{26}\mathrm{Al}}} \sigma_{^{10}\mathrm{B}}(E_n),$$

L. De Smet et al. Phys. Rev. C76 045084

DRESDEN concept HZDR

Frisch-Grid Ionisation Chamber

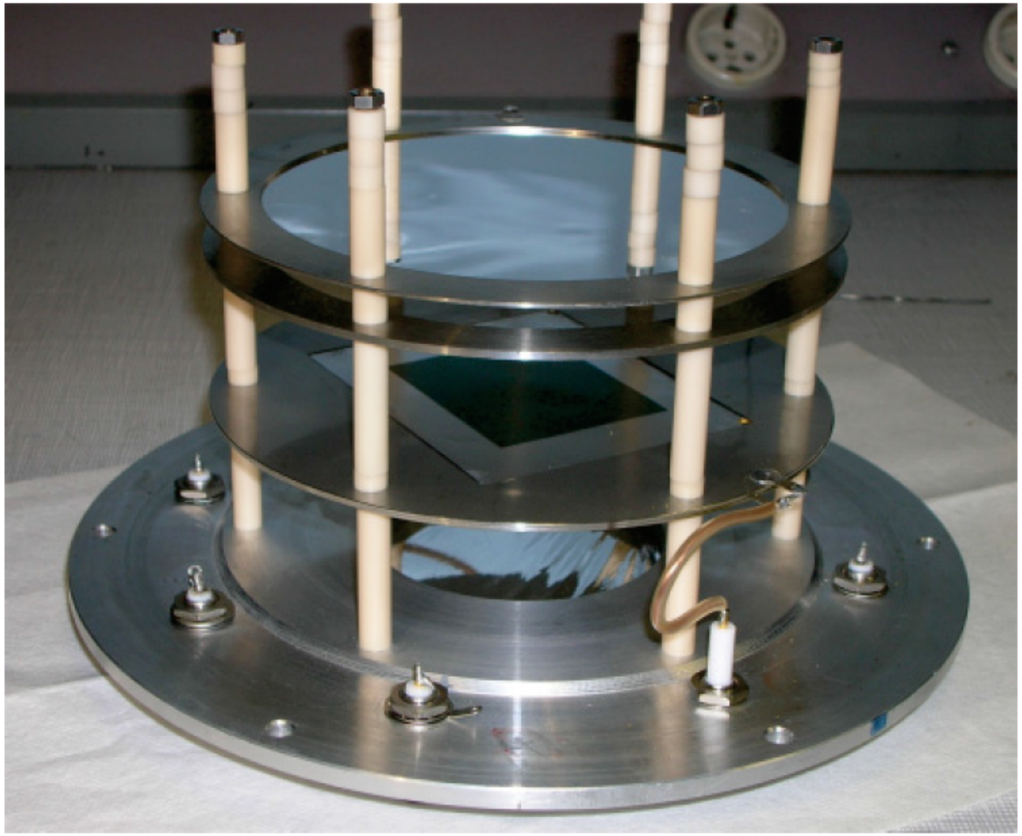

FIG. 1. (Color online) Frisch gridded ionization chamber used in this work. The sample is mounted in the middle of the cathode, which is the lowest plate in the picture. The top plate is the anode; the plate in the middle is the Frisch grid.

2π detection geometry for alphas

Counting gas:
ultrapure methane

L. De Smet et al. Phys. Rev. C76 045084

$^{26}Al(n,\alpha)$ resonances

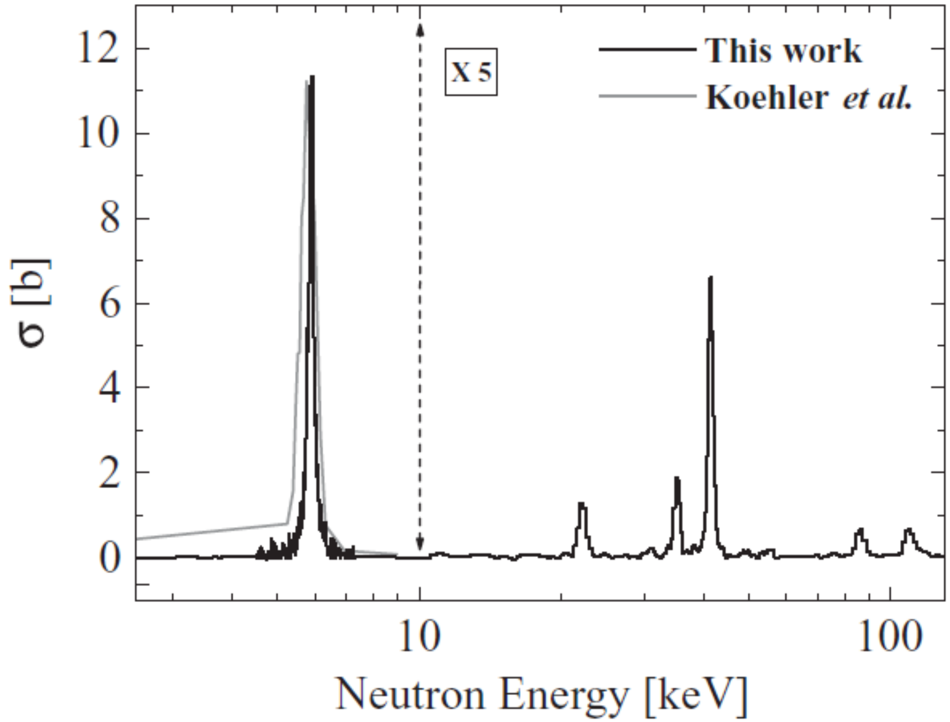

FIG. 5. $^{26}Al(n, \alpha_0 + \alpha_1)^{23}Na$ cross section determined in this work (black line) compared with the $^{26}Al(n, \alpha_0)^{23}Na$ cross section obtained by Koehler *et al.* [11] (gray line).

From the resonant cross section maxwellian averaged cross sections for Nuclear astrophysics can be deduced. → Lecture by R. Reifarth

L. De Smet et al. Phys. Rev. C76 045084

DRESDEN concept

HZDR

Activation measurements of radioactive targets: Irradiation with neutrons in the energy range of 7.5 to 12.5 MeV

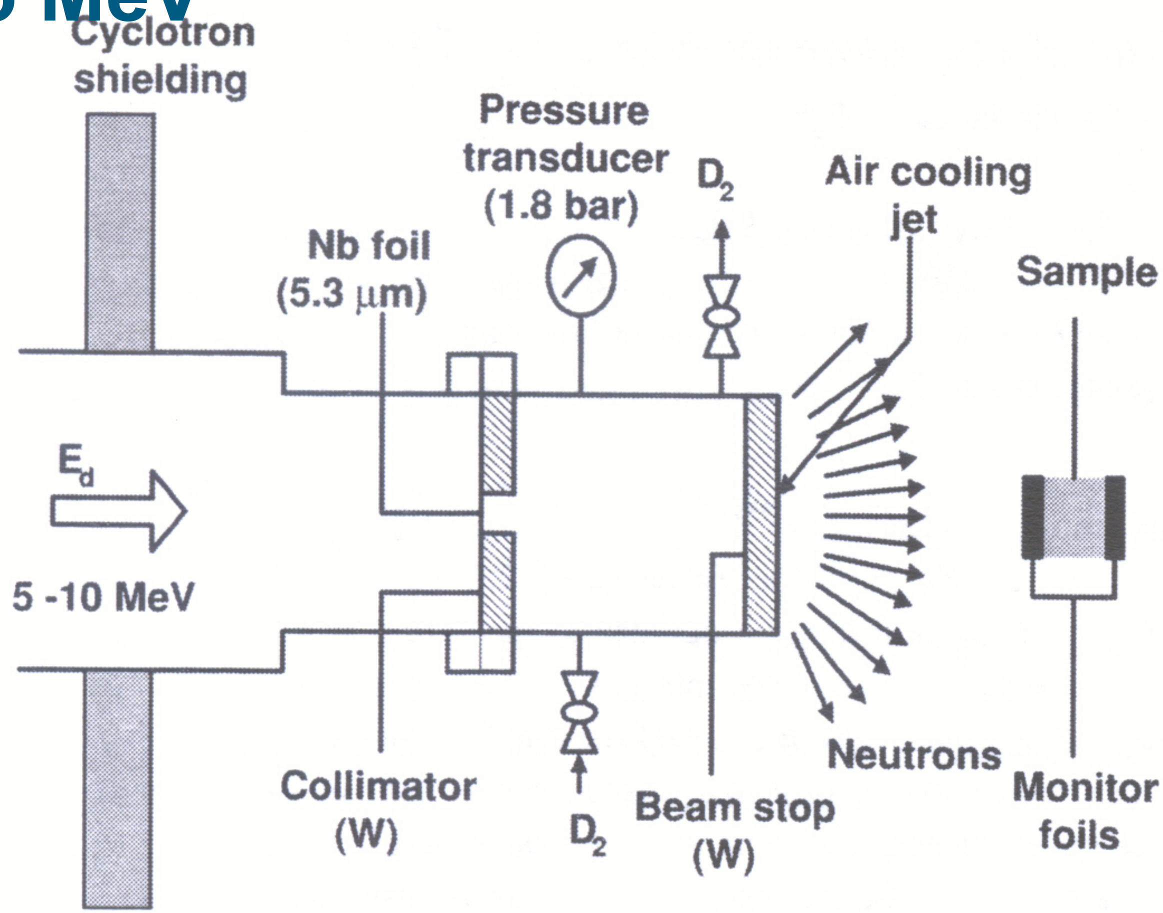

- Background correction via gas in/out experiments

courtesy: Syed M. Quaim, Bad Honneff Seminar 2013

Gas Production in Structural Materials

JÜLICH FORSCHUNGSZENTRUM

Example: $^{58}Ni(n,\alpha)^{55}Fe$ ($T_{1/2}$ = 2.7 a; 5.9 keV X-ray)

Technique: Long irradiation; radiochemical separation of ^{55}Fe; X-ray spectroscopy

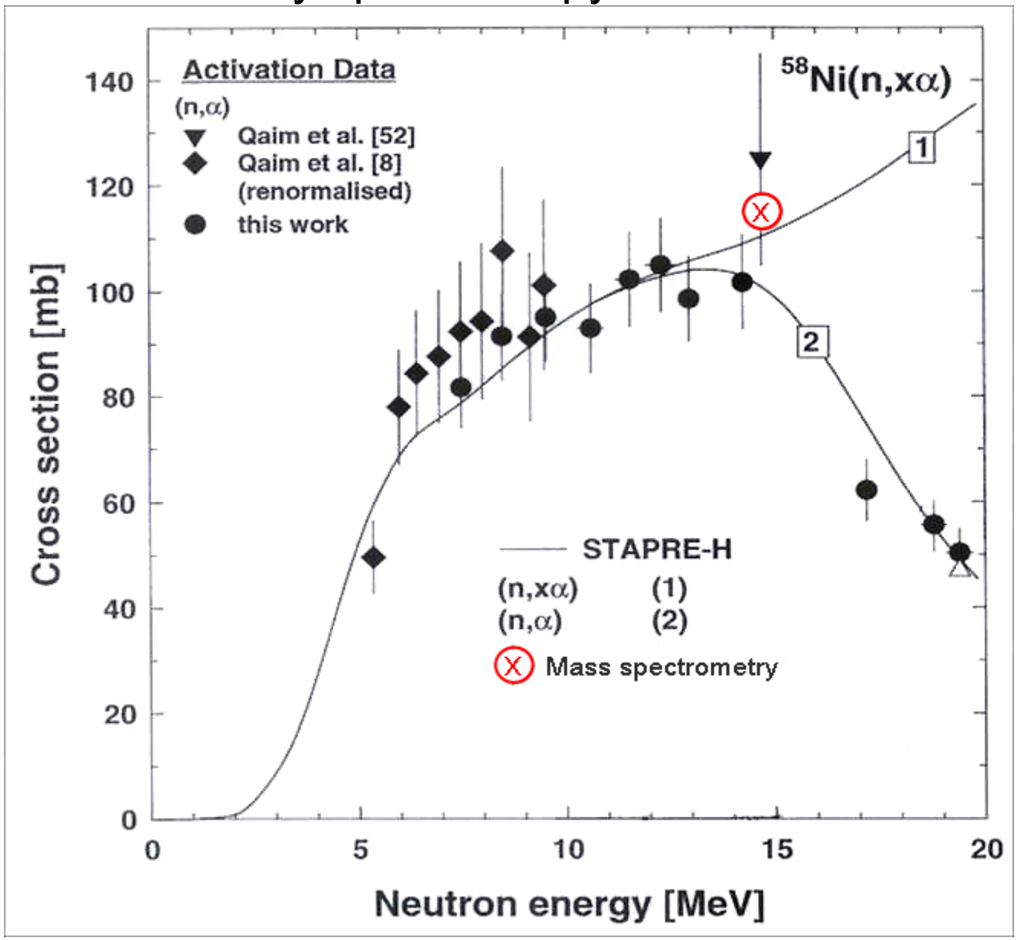

Qaim et al.,

NSE **88**, 143 (1984);

Fessler and Qaim

RCA **84**, 1 (1999).

Comparison of radiochemical data with mass spectrometric data and model calculations adds more confidence to results

Measurements on Radioactive Targets (cont´d)

Example : $^{99}Tc(n,p)^{99}Mo$ ($T_{½}$ = 66.0 h)

Technique : Tc metal (0.5 g) pressed to disc of 13 mm diameter, placed in 0.2 mm thick Al container, sealed in polyethylene bag, attached monitor foils, irradiations with 8 – 20 MeV neutrons. High-resolution γ-ray spectrometry.

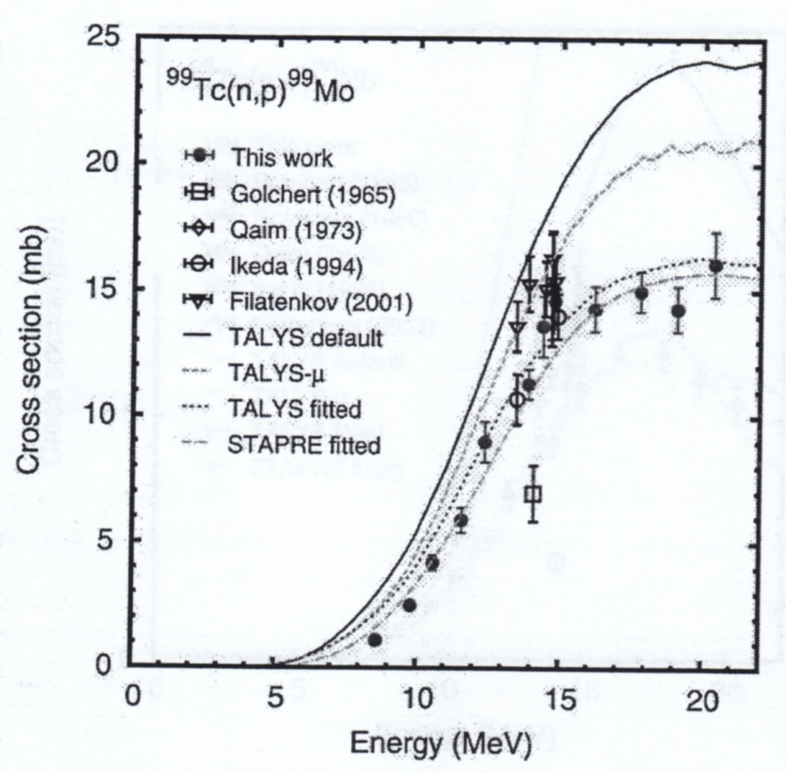

Reimer et al.,
Nucl. Phys. A **815**, 1 (2009)

(Geel – Jülich – Petten – Debrecen collaboration)

- **Database extended**
- **Good test of model calculations**